

miR	p†	FDR (%)‡	Fold change	Chromosomal location	Gastric signature§	Proved targets	Cancer involvement¶
(Continued from previous page)							
MicroRNAs downregulated in cancer							
miR-148a	<1×10 ⁻⁷	<0.01	0.2	7p15.2	..	NR112 (PXR), DNMT3B, TGIF2	Lung, pancreas, prostate
miR-148b	<1×10 ⁻⁷	<0.01	0.3	12q13.13	Histotype	DNMT3B	Colon, lung, pancreas, prostate
miR-375	<1×10 ⁻⁷	<0.01	0.3	2q35	..	JAK2, MTPN, C1QBP, USP1, ADIPOR2, PDK1, AIFM1, RASD1, EEF1E1, GPHN, ELAVL4, CADM1, PLAG1	Pancreas
miR-29b-1, miR-29b-2	1×10 ⁻⁴	<0.01	0.7	7q32.3, 1q32.2	Histotype	TCL1A, DNAJB11, SFPQ, MCL1, DNMT3A, DNMT3B, INSIG1, CAV2, BACE1, COL1A1, COL1A2, COL3A1, FBN1, ELN, YY1, PIK3R1 (p85-ALPHA), CDC42, COL4A2, COL5A3, HDAC4, TGFB3, ACVR2A, DUSP2, CTNBP1	Breast, colon, lung, pancreas, prostate, thyroid, uterus, AML
miR-29c	1×10 ⁻⁵	0.01	0.7	1q32.2	Histotype	DNMT3A, DNMT3B, INSIG1, CAV2, COL1A1, COL1A2, COL3A1, COL4A1, COL4A2, COL15A1, SFRS13A, LAMC1, SPARC, TDG, YY1, PIK3R1 (p85-ALPHA), CDC42	Breast, pancreas, liver, thyroid, oesophagus, nasopharyngeal
miR-152	1×10 ⁻⁵	0.01	0.7	17q21.32	Histotype, progression	..	Pancreas
miR-218-2	2×10 ⁻⁵	<0.01	0.6	5q34	Histotype, progression	LAMB3, MAFG	Lung, pancreas, prostate, stomach, liver, uterus
miR-451	6×10 ⁻⁵	<0.01	0.4	17q11.2	..	GATA2, ABCB1 (MDR1), MIF	..
miR-30d	7×10 ⁻⁵	<0.01	0.7	8q24.22	Histotype	..	Lung, pancreas, thyroid, uterus
miR-30a-5p	7×10 ⁻⁵	0.06	0.7	6q13	..	NOTCH1, BDNF, BECN1	Lung, pancreas, prostate, thyroid
miR-30b	8×10 ⁻⁵	0.06	0.7	8q24.22	Progression	..	Pancreas, prostate, uterus, lymphoma
miR-30c-1, miR-30c-2	0.0003	0.2	0.7	1p34.2, 6q13	Histotype, progression	CTGF, RUNX1 (AML1), UBE2I	Breast, colon, pancreas, prostate
miR-422b	0.0008	0.5	0.7	5q32	Progression

FDR=false discovery rate. AML=acute myeloid leukaemia. CLL=chronic lymphocytic leukaemia. *These microRNAs were used in the clustering of webfigure 1. †Paired class comparison. ‡1% FDR predicts that this list is 99% accurate. §Similarities in gastric cancer signature and other (histotype, progression, and prognostic) signatures. ||Information obtained from Tarbase (<http://diana.cslab.ece.ntua.gr/tarbase>), miRRecords (<http://mirrecords.umn.edu/miRRecords>), and previous reports.^{15,22,24,29,30,31} ¶Information obtained from previous reports.^{24,26,32-35}

Table 2: Frequent differentially expressed microRNAs (gastric cancer signature)*

covariates that were associated significantly with survival (Wald statistic, $p < 0.05$). We tested proportional-hazard assumption by the log-minus-log plot, and no covariate violated assumption. All p values reported are two-sided.

Role of the funding source

The sponsor had no role in study design, data collection, data analysis, data interpretation, writing of the report, or in the decision to submit for publication. The corresponding author had full access to all the data in the study and had final responsibility for the decision to submit for publication.

Results

81 gastric cancer samples (from 79 patients; one patient had cancer in three regions) were obtained at the University of Tokyo (group 1) and 103 samples were gathered at Hiroshima University (group 2) for microRNA expression profiling. Corresponding non-tumour mucosae were available for analysis for 61 cancers in group 1 and 99 in group 2. We also obtained three additional samples of non-tumour mucosa in group 1 and six in group 2, making 353 samples in total—184 cancers and 169 non-tumour mucosae.

Clinical features of patients and tumours are described in table 1 and the webappendix. Disease outcome was known for 101 patients who underwent curative surgery; 42 recurred and died of cancer within the follow-up

period. The final follow-up date was Feb 25, 2007 (median follow-up 785 days [range 159–3070]). Most patients (disease stages IB–IV) were given anticancer drugs either orally or intravenously postoperatively as adjuvant chemotherapy. After disease recurrence, these individuals were given other anticancer drugs.

On microarray analysis, 35 microRNAs were expressed differentially in the paired non-tumour mucosa and cancer samples in groups 1 and 2 (table 2): 22 of these were upregulated and 13 were downregulated in cancer (designated as the gastric cancer signature). By paired class prediction, 97% of samples in group 1 and 94% in group 2 were classified correctly.

On the basis of the 35 microRNAs expressed differentially, cluster analysis with Pearson correlation of the 169 non-tumour mucosa and 184 cancer samples generated a tree showing good separation between non-tumour mucosa and cancer (page 4 of the webappendix). Despite the unpaired condition, 83% (292/353) of samples were classified correctly to non-tumour mucosa or cancer branches.

By quantitative reverse transcription-PCR (qRT-PCR), we analysed 24 pairs of samples investigated initially by microarray for miR-21 (upregulated) and miR-375 (downregulated). We compared the cancer:non-tumour mucosa expression ratio in qRT-PCR with that in the microRNA microarray. The microarray data were confirmed by qRT-PCR (page 5 of the webappendix).

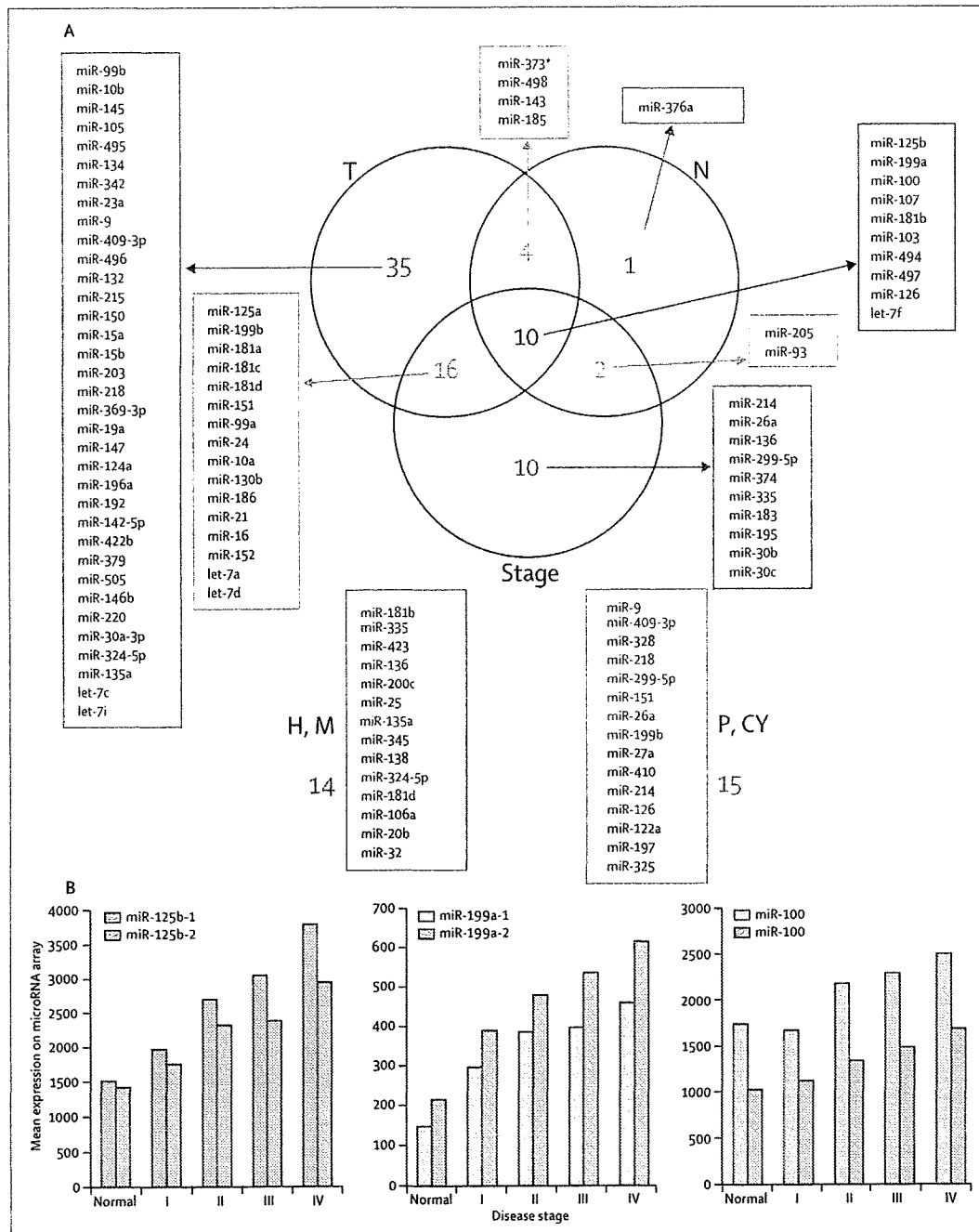


Figure 1: MicroRNAs associated with progression of gastric cancer
 (A) Venn diagram of microRNAs related to T (depth of invasion), N (lymph-node metastasis), and stage. Listed microRNAs comprise the progression signature. Numerals indicate the number of microRNAs. Molecules corresponding to every part of the Venn diagram are shown. MicroRNAs in H and M (haematogenous metastasis) and P and CY (peritoneal dissemination) that are similar to those for T, N, or stage are shown in red. (B) Mean expression levels of miR-125b, miR-199a, and miR-100 on microRNA array according to progression in disease stage. Mean expression levels are shown as linear-scale data on microRNA array analysed with GenePix Pro 6.0; the calculation is based on the intensity (brightness) of each pixel on the microarray image. Mean expression levels of non-tumour mucosa (Normal) of group 1 are also shown. miR-125b-1 and miR-125b-2 are located on different chromosomes but the sequence of mature microRNA is the same; miR-199a-1 and miR-199a-2 are also the same. For miR-100, two probes were included on the microRNA array.

	Univariate analysis		Multivariable analysis†	
	Hazard ratio (95% CI)	p	Hazard ratio (95% CI)	p
Age	1.0 (0.9-1.0)	0.47
Sex				
Men	1.0 (reference)	0.33
Women	1.3 (0.7-2.5)		..	
Histological type				
Intestinal	1.0 (reference)	0.63
Diffuse	1.1 (0.6-2.1)		..	
T				
T1-T2	1.0 (reference)	0.001
T3-T4	3.0 (1.5-6.0)		..	
N				
Negative	1.0 (reference)	<0.0001
Positive	6.0 (2.3-15.5)		..	
Stage				
I-II	1.0 (reference)	<0.0001	1.0 (reference)	<0.0001
III-IV	5.2 (2.5-10.6)		4.3 (2.0-9.2)	
let-7g expression				
High	1.0 (reference)	0.003	1.0 (reference)	0.002
Low	2.6 (1.3-4.9)		2.9 (1.4-6.0)	
miR-214 expression				
Low	1.0 (reference)	0.007	1.0 (reference)	0.004
High	2.4 (1.2-4.5)		2.7 (1.3-5.6)	
miR-433 expression				
High	1.0 (reference)	0.015	1.0 (reference)	<0.0001
Low	2.1 (1.1-3.9)		3.4 (1.7-6.6)	
let-7e expression				
High	1.0 (reference)	0.009
Low	2.2 (1.2-4.2)		..	
let-7i expression				
High	1.0 (reference)	0.039
Low	1.9 (1.0-3.5)		..	

*One patient was censored before first event (patient's death) and these data were removed. †For the final model of multivariable analysis, stage, let-7g, miR-214, and miR-433 were included.

Table 3: Univariate and multivariable Cox regression analysis of overall survival*

The similarity of the microRNA signature in groups 1 and 2 enabled us to merge all samples (184 cancers) into one group for further analyses. 103 diffuse-type and 81 intestinal-type specimens were used to establish whether microRNAs are differentially expressed between histological subtypes. By class comparison, 78 microRNAs were selected (false-discovery rate $\leq 0.42\%$), designated as the histotype signature.

We used the 19 most significant microRNAs (page 9 of the webappendix) in the histotype signature and undertook cluster analysis on the 184 cancer samples. These molecules were selected because they were identified also by SAM in the same order according to the absolute value of the SAM score (data not shown). Even though the histological characteristics of gastric cancer are complex (including seven histological types and mixtures of types), 74% (137/184) of tumours were

distinguished successfully by the expression pattern of these 19 microRNAs (page 6 of the webappendix). Cluster analysis indicated that miR-105, miR-100, miR-125b, miR-199a, miR-99a, miR-143, miR-145, and miR-133a are upregulated in diffuse-type gastric cancer, and miR-373*, miR-498, miR-202*, and miR-494 are upregulated in intestinal-type lesions. These microRNAs are those expressed most differentially, characterising diffuse-type and intestinal-type tumours.

Next, we investigated the correlation between microRNA expression and gastric cancer progression. To identify microRNAs related to progression for every clinical feature, class comparisons were undertaken. 65 microRNAs were selected for T, 17 for N, 14 for H and M, 15 for P and CY, and 38 for stage (figure 1 A). False-discovery rate was 3.3% or less for T, 10.5% for N, 18.8% for P and CY, and 6.9% for stage. Because patients who have distant metastasis undergo surgery rarely, the sample number for positive H and M is just 12. This low number caused a reduction in power to detect microRNAs expressed differentially and a high false-discovery rate. However, six of 14 microRNAs were selected in T, N, or stage (shown in red in figure 1 A), and miR-25, miR-106a, miR-20b, miR-181b, miR-181d, and miR-135a—which were upregulated in gastric cancer relative to non-tumour mucosa—were also chosen. To identify the most important microRNAs associated with progression, we chose T and N as representative progression features and compared them with stage. Ten microRNAs—miR-125b, miR-199a, miR-100, miR-107, miR-181b, miR-103, miR-494, miR-497, miR-126, and let-7f—correlated with these variables (figure 1 A).

By SAM with rank-regression option, we selected 28 microRNAs whose expression was associated with progression from T1 to T4 and 47 microRNAs associated with progression from stage I to IV (data not shown). The q values in SAM of these microRNAs were 0% for T and 1.1% for stage. By comparison of these microRNAs with the ten identified in the previous step, we recorded miR-125b, miR-199a, and miR-100 as the most important microRNAs related to progression of gastric cancer. These three microRNAs showed increasing expression levels according to stage progression (figure 1 B).

We investigated the correlation between microRNA expression profiles and prognosis to establish the microRNAs that might signify unfavourable prognosis (independent of clinical factors). We used samples from 101 patients who underwent curative surgery and their associated prognostic information. Univariate Cox proportional hazards regression indicated that ten microRNAs (let-7c, let-7e, let-7g, let-7i, miR-19a, miR-214, miR-410, miR-433, miR-452, and miR-495) were related to overall survival of patients with gastric cancer. Kaplan-Meier survival curves were generated for every microRNA, and five (let-7e [p=0.007], let-7g [p=0.002], let-7i [p=0.038], miR-214 [p=0.005], and miR-433 [p=0.015]) were associated significantly with survival.

Table 3 shows univariate Cox proportional hazards regression analysis of overall survival relative to clinical factors. T, N, and stage were associated significantly with overall survival, as were five microRNAs. To elucidate whether these microRNAs are independent prognostic factors, multivariable analysis was done. The dichotomised expression values of these five microRNAs were not associated with clinical factors (Fisher's exact test). Because T and N were associated highly with stage by Fisher's exact test, and the same microRNAs were chosen in the final model of multivariable analysis including stage and in the final model including T and N, we showed only the stage model (table 3). In the final multivariable model, let-7g, miR-214, and miR-433 were associated with overall survival independent of clinical covariates (table 3). Patients with low expression of let-7g (hazard ratio 2.6 [95% CI 1.3–4.9]), low expression of miR-433 (2.1 [1.1–3.9]), or high expression of miR-214 (2.4 [1.2–4.5]) had poorer survival than did patients with high expression of let-7g, high expression of miR-433, or low expression of miR-214 (figure 2).

We validated the results for let-7g and miR-214 by qRT-PCR. 12 samples selected from the low-expression group showed low expression of let-7g and miR-214 by qRT-PCR, and 12 samples selected from the high-expression group showed high expression (page 7 of the webappendix). We analysed three additional specimens by qRT-PCR that were not used in microRNA array analysis because of low RNA yield. One sample with an unfavourable outcome showed high expression of miR-214 (higher than the mean of 12 samples from the high-expression group), and two with a favourable outcome showed low expression of miR-214 (lower than the mean of 12 samples from the low-expression group), consistent with our results.

We undertook the same analyses for disease-free survival in 101 patients. By univariate Cox proportional hazards regression, 12 microRNAs (let-7b, let-7c, let-7d, let-7g, miR-19a, miR-196a, miR-220, miR-373, miR-410, miR-433, miR-452, and miR-495) were related to disease-free survival of patients with gastric cancer. By log-rank analysis, six microRNAs (let-7b [$p=0.001$], let-7g [$p=0.001$], miR-19a [$p=0.031$], miR-410 [$p=0.015$], miR-433 [$p=0.011$], and miR-495 [$p=0.035$]) were related to survival. On univariate analysis, T, N, stage, and these six microRNAs were associated significantly with disease-free survival (table 4). The dichotomised expression values of six microRNAs were not associated with clinical factors (Fisher's exact test). Because T and N were associated highly with stage by Fisher's exact test, and the same microRNAs were chosen in the final model of multivariable analysis including stage and in the final model including T and N, we showed only the stage model (table 4). In the final multivariable Cox regression model, let-7b, let-7g, miR-19a, and miR-495 were associated with disease-free survival independent of clinical covariates (table 4). In

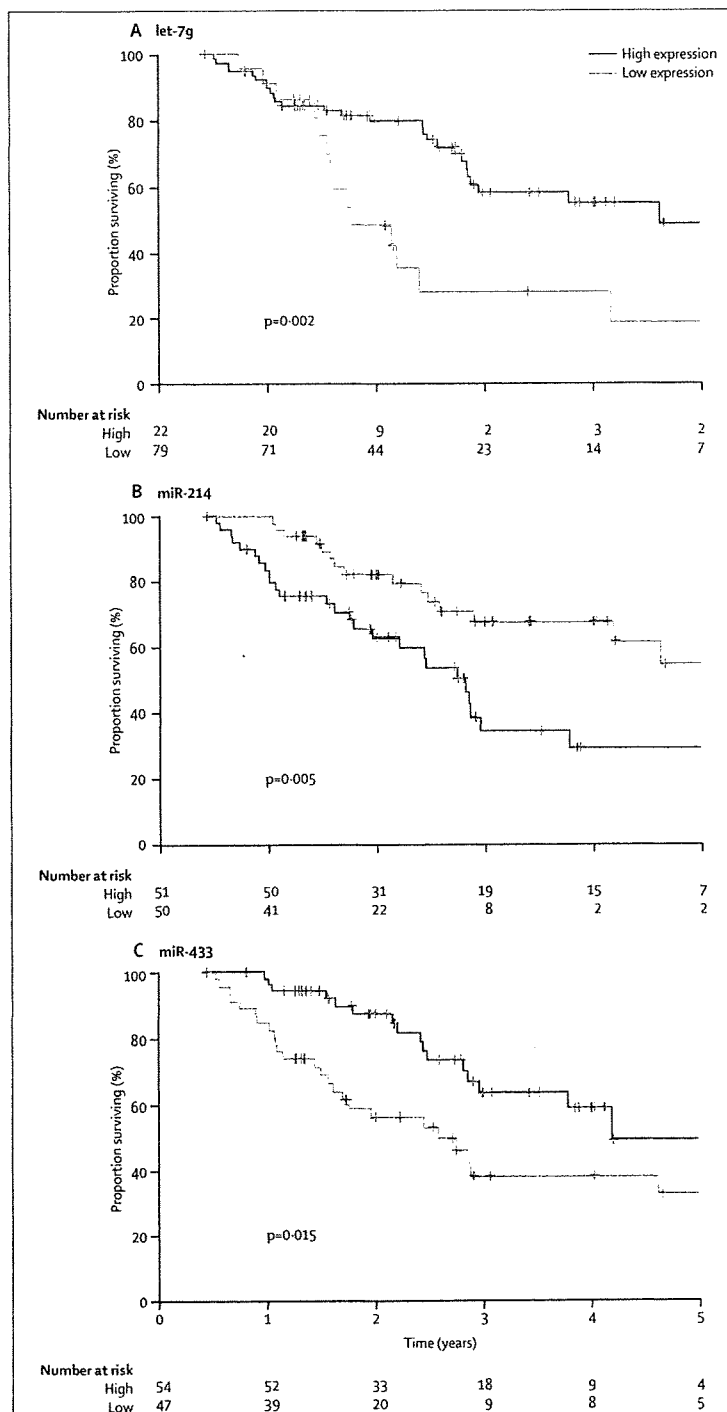


Figure 2: Kaplan-Meier curves of independent prognostic factors for overall survival. Curves are depicted with data for 101 patients. MicroRNA expression levels measured on the microarray were converted into discrete variables by division of samples into two classes (high and low expression), with the respective mean levels of microRNA expression as a threshold. Censored cases are shown on the curves. p values are log rank.

	Univariate analysis		Multivariable analysis†	
	Hazard ratio (95% CI)	p	Hazard ratio (95% CI)	p
Age	1.0 (0.9-1.0)	0.63
Sex				
Men	1.0 (reference)	0.31
Women	1.3 (0.7-2.5)		..	
Histological type				
Intestinal	1.0 (reference)	0.67
Diffuse	1.1 (0.6-2.1)		..	
T				
T1-T2	1.0 (reference)	0.001
T3-T4	3.1 (1.5-6.1)		..	
N				
Negative	1.0 (reference)	<0.0001
Positive	5.5 (2.1-14.2)		..	
Stage				
I-II	1.0 (reference)	<0.0001	1.0 (reference)	<0.0001
III-IV	4.5 (2.2-9.2)		5.2 (2.4-11.2)	
let-7b expression				
High	1.0 (reference)	0.003	1.0 (reference)	0.001
Low	2.7 (1.4-5.4)		3.2 (1.6-6.6)	
let-7g expression				
High	1.0 (reference)	0.002	1.0 (reference)	0.042
Low	2.7 (1.4-5.2)		2.0 (1.0-3.9)	
miR-19a expression				
High	1.0 (reference)	0.032	1.0 (reference)	<0.0001
Low	2.0 (1.0-3.6)		3.3 (1.7-6.5)	
miR-495 expression				
Low	1.0 (reference)	0.035	1.0 (reference)	0.007
High	1.9 (1.0-3.6)		2.4 (1.2-4.7)	
miR-410 expression				
Low	1.0 (reference)	0.016
High	2.2 (1.1-4.3)		..	
miR-433 expression				
High	1.0 (reference)	0.011
Low	2.1 (1.1-4.0)		..	

*No patients were censored before first event (disease recurrence). †For the final model of multivariable analysis, stage, let-7b, let-7g, miR-19a, and miR-495 were included.

Table 4: Univariate and multivariable Cox regression analysis of disease-free survival*

both overall survival and disease-free survival, let-7g was selected as an independent prognostic factor (tables 3 and 4).

101 patients were divided into two groups by histological type (intestinal and diffuse) and multivariable Cox proportional hazards regression analysis was undertaken in the same way. The selected microRNAs remained as independent prognostic factors (table 5).

Discussion

Aberrant microRNA expression patterns have been described in various haematological and solid cancers,^{14-16,20-22} and alterations in microRNA expression correlate highly with progression and prognosis of human

malignant diseases.¹⁵⁻²⁴ However, profiles of microRNAs differ and need to be investigated in every type of tumour. In this study, we recorded substantial associations between differential expression of specific microRNAs and progression and prognosis of gastric cancer.

Antiapoptotic miR-21 is upregulated in various solid cancers and is related to tumour growth.^{15,30} In previous work, miR-21 was overexpressed in gastric cancer and in *Helicobacter pylori*-infected gastric mucosa.³⁰ *H pylori* is an important pathogen for gastric cancer, and data are already starting to suggest the molecular mechanism of evolution of normal mucosa to chronic gastritis, atrophic gastritis, and intestinal metaplasia. Our sample set contained no detailed information about *H pylori* infection status because pathologists recorded histological types, depth of invasion, and status of lymph-node metastasis to decide clinical stage of cases. Non-tumour mucosae were obtained during surgery from resected stomach that seemed to be normal macroscopically. Therefore, in this study we could not investigate the correlation between microRNA expression and *H pylori* or chronic gastritis; however, we will investigate this important area in further studies.

We identified 35 differentially expressed microRNAs without use of microdissection. This procedure is difficult to adapt to some diffuse-type gastric cancers because cancer cells are localised singly. In a previous report, we analysed by microarray 20 pairs of intestinal-type gastric cancer and non-tumour mucosa samples from a white population and noted 14 upregulated and five downregulated microRNAs in cancers.³¹ All the upregulated microRNAs and three of those downregulated (60%) were similar to the molecules selected in this study, meaning that our method of using bulk samples of diffuse-type gastric cancer for microarray analysis can produce correct results, although they must be validated by in-situ hybridisation. This result also means that despite patients' different ethnic backgrounds in this and our previous study, the microRNA signature is linked to general mechanisms of gastric cancer tumorigenesis.

For some of the microRNAs we identified in gastric cancer samples, several targets have already been proven experimentally. We showed previously that molecules expressed differentially in the microRNA cluster miR-106b-25 are related to gastric cancer tumorigenesis,³¹ suggesting that microRNAs have important roles in gastric cancer. Although gastric cancer is histologically complex and sometimes shows transition from differentiated to undifferentiated subtypes in the same tumour (ie, mixed type), we divided samples into diffuse and intestinal types and identified microRNAs expressed differentially, characterising these histological classes. A collaborator of ours reported that the Hedgehog signal is more active in diffuse-type than intestinal-type gastric cancer,³¹ and glioma-associated oncogene homologue 1 (*GLI1*), a downstream target of the Hedgehog signal, is

an in-silico target of miR-373*, which is downregulated in diffuse-type gastric cancer.

In this study, we identified microRNAs related to the progression of gastric cancer. In breast cancer, tumour invasion and metastasis are initiated by miR-10b,²⁴ which is one of the microRNAs associated with invasion in gastric cancer. miR-21 was selected in the progression signature of both T and stage, and it targets programmed cell death 4 (*PDCD4*) and maspin (*SERPIN5*), resulting in tumour invasion and metastasis.²⁴ Another group showed that miR-21 targets a tumour-suppressor gene, reversion-inducing-cysteine-rich protein with kazal motifs (*RECK*), and that knockdown of miR-21 decreased invasion and migration of gastric cancer cells significantly.³⁰ The microRNAs that were related most significantly to progression of gastric cancer—miR-125b, miR-199a, and miR-100—were also upregulated in pancreatic adenocarcinoma in our previous study.²¹ miR-125b is reportedly related to proliferation of differentiated cells³² and downregulated in breast cancer³⁴ and thyroid anaplastic carcinoma,³² suggesting that this microRNA functions differently in gastric cancer and pancreatic adenocarcinoma. Proapoptotic *BAK1* and *TP53* are proven targets of miR-125b in prostate cancer and neuroblastoma cells, supporting the oncogenic function of miR-125b.^{34,35} Upregulation of miR-199a is associated purportedly with tumour cell growth in cervical carcinoma.³⁶

We identified microRNAs associated with an unfavourable outcome (independent of clinical factors) in specimens from patients treated by curative surgery and adjuvant chemotherapy. Although our findings should be validated in an independent cohort, these microRNAs might help to identify individuals who are candidates for aggressive treatment because of their expression status and who could become candidates for therapeutic targets with antagonists²⁵⁻²⁷ or by reconstitution with microRNA precursor sequences.²⁸ Three microRNAs selected in the progression analysis were not chosen for the prognostic signature partly because they were associated highly with clinical factors. The difference of the selected microRNAs between overall and disease-free survival is probably caused by the effect of chemotherapy after disease recurrence.

We chose let-7g and let-7b as independent prognostic factors. The Ras family of oncogenes is regulated by the let-7 family in lung cancer,^{37,38} and the high mobility group AT-hook 2 (*HMGAT2*) oncogene is also targeted by this microRNA family.^{37,38} *HMGAT2* is regulated negatively by the let-7 family, and high expression of this gene correlates with tumour invasiveness and is an unfavourable prognostic factor in gastric cancer.³⁹ Additionally, in tumour-initiating cells of breast cancer (which have stem cell-like properties), let-7 regulates self-renewal (by silencing *HRAS*) and differentiation (by silencing *HMGAT2*).²⁴ Administration of let-7 family members inhibits growth of lung cancer in mice.^{37,38} A negative regulator of hedgehog signalling, suppressor of fused

	Hazard ratio (95% CI)	p
Disease-free survival		
Intestinal type (n=45)		
Stage, III-IV vs I-II*	3.2 (1.1-9.1)	0.032
let-7g expression, low vs high*	2.8 (1.0-7.8)	0.043
miR-19a expression, low vs high*	7.5 (2.3-24.6)	0.001
miR-495 expression, high vs low*	4.9 (1.7-14.3)	0.004
Diffuse type (n=56)		
Stage, III-IV vs I-II*	5.5 (1.9-15.7)	0.001
let-7b expression, low vs high*	2.6 (1.1-6.2)	0.031
Overall survival*		
Intestinal type (n=45)		
Stage, III-IV vs I-II*	5.7 (2.0-16.0)	0.001
miR-433 expression, low vs high*	4.4 (1.6-12.2)	0.004
Diffuse type (n=55)		
Stage, III-IV vs I-II*	6.3 (2.1-18.9)	0.001
miR-214 expression, high vs low*	2.7 (1.0-7.3)	0.048
miR-433 expression, low vs high*	2.4 (1.0-5.6)	0.050

*Reference group. For all microRNAs, patients were categorised into high-expression and low-expression groups with the same cutoff values of microRNA expression used in tables 3 and 4. Multivariable analysis was undertaken by stepwise addition and removal of covariates found to be associated with survival in tables 3 and 4. Only final models are shown. *In overall survival of diffuse-type gastric cancer, one patient was censored before first event (patient's death) and these data were removed.

Table 5: Multivariable Cox regression analysis of disease-free survival and overall survival of patients with intestinal-type and diffuse-type gastric cancer

(*sufl4*), is targeted by miR-214 in the development of zebrafish,⁴⁰ and activation of hedgehog signalling is involved in gastric cancer.³² Recently, miR-214 was reported to induce cell survival and cisplatin resistance by targeting *PTEN* in ovarian cancer.⁴¹ miR-433 targets growth factor receptor-bound protein 2 (*GRB2*) in gastric cancer.⁴²

Further studies are needed to establish whether the microRNAs we selected in this study have full potential as either biomarkers or therapeutic targets in gastric cancer. Proving new targets and other biological experiments will clarify the functions and roles of microRNAs in gastric cancer. However, we have shown already that microRNAs can meet criteria for ideal biomarkers and therapeutic targets.²²

Contributors

All authors planned and implemented the investigation. TU, YS, MK, WY, HS, GAC, and CMC had the idea for and designed the experiments. TU, SN, NO, and KY obtained samples and clinical data. TU, HO, MS, HA, and C-gL undertook the experiments. SV, CT, SR, and TU did the statistical analysis. TU, SV, CT, GAC, and CMC wrote the report. All authors critically reviewed the manuscript and approved the final version.

Conflicts of interest

The authors declared no conflicts of interest.

Acknowledgments

We thank Karen F Phillips (Department of Scientific Publications, University of Texas MD Anderson Cancer Center) for editorial assistance. This research was supported by Program Project Grants from the National Cancer Institute (CMC) and in part by an NIH grant

1R01CA135444. GAC is supported as a fellow at the University of Texas MD Anderson Research Trust, as a fellow of the University of Texas System Regents Research Scholar, and by the Ladjevardian Regents Research Scholar Fund. SV was supported by AIRC and Regione Emilia-Romagna PRRITTT grants.

References

- Parkin DM, Bray F, Ferlay J, Pisani P. Global cancer statistics, 2002. *CA Cancer J Clin* 2005; 55: 74–108.
- Hohenberger P, Gretschel S. Gastric cancer. *Lancet* 2003; 362: 305–15.
- Yasui W, Yokozaki H, Fujimoto J, Naka K, Kuniyasu H, Tahara E. Genetic and epigenetic alterations in multistep carcinogenesis of the stomach. *J Gastroenterol* 2000; 35: 111–15.
- Stock M, Otto F. Gene deregulation in gastric cancer. *Gene* 2005; 360: 1–19.
- Li Q-L, Ito K, Sakakura C, et al. Causal relationship between the loss of *RUNX3* expression and gastric cancer. *Cell* 2002; 109: 113–24.
- Jinawath N, Furukawa Y, Hasegawa S, et al. Comparison of gene-expression profiles between diffuse- and intestinal-type gastric cancers using a genome-wide cDNA microarray. *Oncogene* 2004; 23: 6830–44.
- Lagos-Quintana M, Rauhut R, Lendeckel W, Tuschl T. Identification of novel genes coding for small expressed RNAs. *Science* 2001; 294: 853–58.
- Bartel DP. MicroRNAs: genomics, biogenesis, mechanism, and function. *Cell* 2004; 116: 281–97.
- Krek A, Grun D, Poy MN, et al. Combinatorial microRNA target predictions. *Nat Genet* 2005; 37: 495–500.
- Ambros V. The functions of animal microRNAs. *Nature* 2004; 431: 350–55.
- Griffiths-Jones S, Grocock RJ, van Dongen S, Bateman A, Enright AJ. miRBase: microRNA sequences, targets and gene nomenclature. *Nucleic Acids Res* 2006; 34: D140–44.
- Bentwich I, Avniel A, Karov Y, et al. Identification of hundreds of conserved and nonconserved human microRNAs. *Nat Genet* 2005; 37: 766–70.
- Liu CG, Calin GA, Volinia S, Croce CM. MicroRNA expression profiling using microarrays. *Nat Protoc* 2008; 3: 563–78.
- Iorio MV, Ferracin M, Liu CG, et al. MicroRNA gene expression deregulation in human breast cancer. *Cancer Res* 2005; 65: 7065–70.
- Volinia S, Calin GA, Liu CG, et al. A microRNA expression signature of human solid tumors defines cancer gene targets. *Proc Natl Acad Sci USA* 2006; 103: 2257–61.
- Gramantieri L, Ferracin M, Fornari F, et al. Cyclin G1 is a target of miR-122a, a microRNA frequently down-regulated in human hepatocellular carcinoma. *Cancer Res* 2007; 67: 6092–99.
- Esquela-Kerscher A, Slack FJ. Oncomirs: microRNAs with a role in cancer. *Nat Rev Cancer* 2006; 6: 259–69.
- Calin GA, Croce CM. MicroRNA signatures in human cancers. *Nat Rev Cancer* 2006; 6: 857–66.
- Calin GA, Ferracin M, Cimmino A, et al. A microRNA signature associated with prognosis and progression in chronic lymphocytic leukemia. *N Engl J Med* 2005; 353: 1793–801.
- Yanaihara N, Caplen N, Bowman E, et al. Unique microRNA molecular profiles in lung cancer diagnosis and prognosis. *Cancer Cell* 2006; 9: 189–98.
- Bloomston M, Frankel WL, Petrocca F, et al. MicroRNA expression patterns to differentiate pancreatic adenocarcinoma from normal pancreas and chronic pancreatitis. *JAMA* 2007; 297: 1901–08.
- Schetter AJ, Leung SY, Sohn JJ, et al. MicroRNA expression profiles associated with prognosis and therapeutic outcome in colon adenocarcinoma. *JAMA* 2008; 299: 425–36.
- Garzon R, Volinia S, Liu CG, et al. MicroRNA signatures associated with cytogenetics and prognosis in acute myeloid leukemia. *Blood* 2008; 111: 3183–89.
- Nicoloso MS, Spizzo R, Shimizu M, Rossi S, Calin GA. MicroRNAs: the micro steering wheel of tumour metastases. *Nat Rev Cancer* 2009; 9: 293–302.
- Krützfeldt J, Rajewsky N, Braich R, et al. Silencing of microRNAs in vivo with 'antagomirs'. *Nature* 2005; 438: 685–89.
- Elmén J, Lindow M, Schütz S, et al. LNA-mediated microRNA silencing in non-human primates. *Nature* 2008; 452: 896–99.
- Akinc A, Zumbuehl A, Goldberg M, et al. A combinatorial library of lipid-like materials for delivery of RNAi therapeutics. *Nat Biotechnol* 2008; 26: 561–69.
- Tong AW, Nernunaitis J. Modulation of miRNA activity in human cancer: a new paradigm for cancer gene therapy? *Cancer Gene Ther* 2008; 15: 341–55.
- National Cancer Institute, Biometric Research Branch. BRB-ArrayTools. <http://linus.nci.nih.gov/BRB-ArrayTools.html> (accessed Dec 1, 2009).
- Zhang Z, Li Z, Gao C, et al. miR-21 plays a pivotal role in gastric cancer pathogenesis and progression. *Lab Invest* 2008; 88: 1358–66.
- Petrocca F, Visone R, Onelli MR, et al. E2F1-regulated microRNAs impair TGFβ-dependent cell-cycle arrest and apoptosis in gastric cancer. *Cancer Cell* 2008; 13: 272–86.
- Visone R, Pallante P, Vecchione A, et al. Specific microRNAs are downregulated in human thyroid anaplastic carcinomas. *Oncogene* 2007; 26: 7590–95.
- Fukaya M, Isohata N, Ohta H, et al. Hedgehog signal activation in gastric pit cell and in diffuse-type gastric cancer. *Gastroenterology* 2006; 131: 14–29.
- Shi XB, Xue L, Yang J, et al. An androgen-regulated miRNA suppresses Bcl1 expression and induces androgen-independent growth of prostate cancer cells. *Proc Natl Acad Sci USA* 2007; 104: 19983–88.
- Le MT, Teh C, Shyh-Chang N, et al. MicroRNA-125b is a novel negative regulator of p53. *Genes Dev* 2009; 23: 862–76.
- Lee JW, Choi CH, Choi JJ, et al. Altered microRNA expression in cervical carcinomas. *Clin Cancer Res* 2008; 14: 2535–42.
- Kumar MS, Erkeland SJ, Pester RE, et al. Suppression of non-small cell lung tumor development by the let-7 microRNA family. *Proc Natl Acad Sci USA* 2008; 105: 3903–08.
- Esquela-Kerscher A, Trang P, Wiggins JF, et al. The let-7 microRNA reduces tumor growth in mouse models of lung cancer. *Cell Cycle* 2008; 7: 759–64.
- Motoyama K, Inoue H, Nakamura Y, Uetake H, Sugihara K, Mori M. Clinical significance of high mobility group A2 in human gastric cancer and its relationship to let-7 microRNA family. *Clin Cancer Res* 2008; 14: 2334–40.
- Flynt AS, Li N, Thatcher EJ, Solnica-Krezel L, Patton JG. Zebrafish miR-214 modulates Hedgehog signaling to specify muscle cell fate. *Nat Genet* 2007; 39: 259–63.
- Yang H, Kong W, He L, et al. MicroRNA expression profiling in human ovarian cancer: miR-214 induces cell survival and cisplatin resistance by targeting PTEN. *Cancer Res* 2008; 68: 425–33.
- Luo H, Zhang H, Zhang Z, et al. Down-regulated miR-9 and miR-433 in human gastric carcinoma. *J Exp Clin Cancer Res* 2009; 28: 82.

Serial analysis of gene expression of esophageal squamous cell carcinoma: *ADAMTS16* is upregulated in esophageal squamous cell carcinoma

Naoya Sakamoto,¹ Naohide Oue,¹ Tsuyoshi Noguchi,² Kazuhiro Sentani,¹ Katsuhiko Anami,¹ Yuichi Sanada,³ Kazuhiro Yoshida³ and Wataru Yasui^{1,4}

¹Department of Molecular Pathology, Hiroshima University Graduate School of Biomedical Sciences, Hiroshima; ²Department of Gastrointestinal Surgery, Oita University Faculty of Medicine, Oita; ³Department of Surgical Oncology, Gifu Graduate School of Medicine, Gifu, Japan

(Received October 19, 2009/Revised December 5, 2009/Accepted December 9, 2009)

Esophageal squamous cell carcinoma (ESCC) is one of the most common malignancies worldwide. To identify potential diagnostic markers for ESCC and therapeutic targets for ESCC, we used Serial Analysis of Gene Expression (SAGE) on one ESCC sample. We obtained a total of 14 430 tags, including 5765 that were unique. By comparing SAGE tags from the ESCC sample with those from normal human squamous esophagus, we found several genes that were differentially expressed between ESCC and normal squamous esophagus. Among these, we focused on the ADAM metalloproteinase with thrombospondin type 1 motif, 16 (*ADAMTS16*) gene because quantitative RT-PCR analysis showed a high level of *ADAMTS16* expression in eight out of 20 ESCC samples (40%), but not in 15 kinds of normal tissues. Western blot analysis also showed upregulation of *ADAMTS16* protein in ESCC tissues. Furthermore, *ADAMTS16* protein was detected in culture media from the TE5 esophageal cancer cell line. Knockdown of *ADAMTS16* in TE5 cells inhibited both cell growth and invasion ability. Our present SAGE data provide a list of genes potentially associated with ESCC. *ADAMTS16* could be a novel diagnostic and therapeutic target for ESCC. (*Cancer Sci* 2010)

Human esophageal cancer occurs worldwide with a variable geographic distribution and ranks eighth in order of occurrence and sixth as a leading cause of cancer mortality, affecting men more than women.⁽¹⁾ There are two main forms, each with distinct etiologic and pathologic characteristics, esophageal squamous cell carcinoma (ESCC) and adenocarcinoma. ESCC is the most frequent subtype of esophageal cancer, although the incidence of adenocarcinoma in the USA and UK is increasing faster than other esophageal malignancies. Most ESCC is diagnosed at an advanced stage, and even superficial ESCC that appears to extend no further than the submucosa metastasizes to the lymph nodes in 50% of cases.⁽²⁾ In spite of the use of modern surgical techniques combined with various treatment modalities, such as chemoradiotherapy (CRT), the overall 5-year survival rate of ESCC still remains at 40–60%.⁽³⁾ Therefore, identification of new diagnostic markers for ESCC and new therapeutic targets for ESCC is important.

Better knowledge of changes in gene expression that occur during carcinogenesis might lead to improvements in diagnosis, treatment, and prevention of ESCC. Genes encoding transmembrane/secretory proteins expressed specifically in cancers may be ideal diagnostic biomarkers.⁽⁴⁾ Moreover, if the gene product functions in the neoplastic process, the gene is not just a biomarker but might also be a therapeutic target.⁽⁵⁾ To identify potential markers for early detection of ESCC and therapeutic targets for ESCC, comprehensive gene expression analysis could be useful. Studies on differential global gene expression profiling in ESCCs using cDNA and oligonucleotide arrays have been carried

out in various populations.^(6,7) Although many studies have been done on gene expression profiling of specific tumor types, and differentially expressed genes in these tumors have been reported, few of these studies have resulted in clinical applications. However, among the comprehensive methods used to analyze transcript expression levels, Serial Analysis of Gene Expression (SAGE) is a common approach.⁽⁸⁾ We previously carried out SAGE on four primary gastric cancer tissues⁽⁹⁾ and identified several gastric cancer-specific genes.⁽¹⁰⁾ Of these genes, regenerating islet-derived family, member 4 (*REG4*, which encodes Reg IV) and olfactomedin 4 (*OLFM4*, also known as GW112 or hGC-1) are highly sensitive serum markers for gastric cancer.^(11,12) However, SAGE analysis on ESCC tissue has been done in only one case.⁽¹³⁾

In the present study, we generated the SAGE library from one ESCC sample. By comparing SAGE tags from ESCC samples with those from normal human squamous esophagus (Gene Expression Omnibus accession number, GSM52501),⁽¹⁴⁾ we found several genes and tags that were differentially expressed between ESCC and normal squamous esophagus. Among these, we focused on the ADAM metalloproteinase with thrombospondin type I motif, 16 (*ADAMTS16*) gene because it is frequently overexpressed in ESCC, and *ADAMTS16* expression is narrowly restricted among various normal tissues. In addition, the amino acid sequence of the *ADAMTS16* protein suggests that it might be secreted. *ADAMTS* has been described as part of a family of zinc-dependent proteases (metzincin family) that play important roles in a variety of normal and pathological conditions, including arthritis and cancer.^(15,16) Although expression of *ADAMTS16* in some organs has been reported, the relationship with cancers, including ESCC, has not been studied.

Materials and Methods

Tissue samples. For SAGE analysis, one primary ESCC (75-year-old male, T2N0M0) sample was used (Fig. 1). We confirmed microscopically that the tumor specimens consisted mainly (>80%) of carcinoma tissue. For quantitative RT-PCR analysis, 20 ESCC tissue samples and corresponding non-neoplastic mucosa samples were used. For Western blot analysis, four ESCC tissue samples and corresponding non-neoplastic mucosa samples were used. The samples were obtained from surgeries at Hiroshima University Hospital and affiliated hospitals. Samples were frozen immediately in liquid nitrogen and stored at –80°C until use. Fifteen kinds of normal tissue samples, including heart, lung, esophagus, stomach, small intestine, colon, liver, pancreas, kidney, bone marrow, peripheral

⁴To whom correspondence should be addressed.
E-mail: wyasui@hiroshima-u.ac.jp

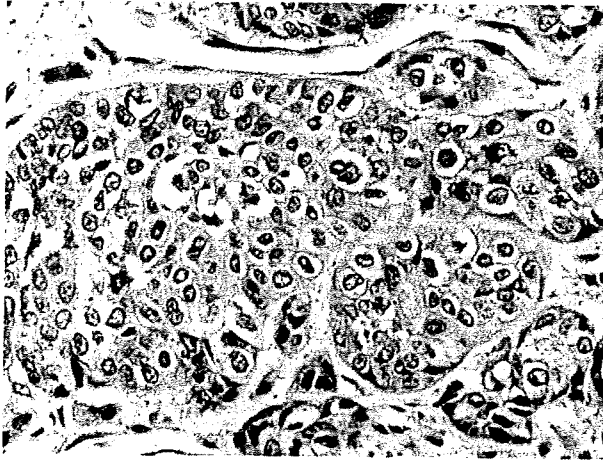


Fig. 1. Histological features of the esophageal squamous cell carcinoma sample analyzed by Serial Analysis of Gene Expression. The formalin-fixed, paraffin-embedded section was stained with H&E.

leukocytes, spleen, skeletal muscle, brain, and spinal cord, were purchased from Clontech (Palo Alto, CA, USA). Histological classification was based on the World Health Organization system. Tumor staging was done according to the TNM stage grouping system.⁽¹⁷⁾ For strict privacy protection, identifying information for all samples was removed before analysis. This procedure was in accordance with the Ethical Guidelines for Human Genome/Gene Research of the Japanese Government.

Serial analysis of gene expression. SAGE was carried out according to SAGE protocol version 1.0e (June 23, 2000). Tags were extracted from the raw sequence data with SAGE2000 analysis software version 4.12, kindly provided by Dr. Kenneth W. Kinzler (Ludwig Center for Cancer Genetics and Therapeutics and Howard Hughes Medical Institute, Johns Hopkins Kimmel Cancer Center, Baltimore, MD, USA).

Quantitative RT-PCR. Total RNA was extracted with an RNeasy Mini Kit (Qiagen, Valencia, CA, USA), and 1 µg total RNA was converted to cDNA with a First Strand cDNA Synthesis Kit (Amersham Biosciences, Piscataway, NJ, USA). PCR was carried out with a SYBR Green PCR Core Reagents Kit (Applied Biosystems, Foster City, CA, USA). *ADAMTS16* primer sequences were 5'-TCT CAT AGG AGT CGC CTC TGC-3' and 5'-CGA GTG GAG CCC TCA CAG AA-3'. Squamous cell carcinoma antigen A1 (*SCCA1*) primer sequences were 5'-GAA TGG TGG ATA TCT TCA ATG GG-3' and 5'-GAT AGC ACG AGA CCG CGG-3'. Real-time detection of the emission intensity of SYBR Green bound to double-stranded DNA was done with an ABI PRISM 7700 Sequence Detection System (Applied Biosystems) as described previously.⁽¹⁸⁾ Actin-beta-specific PCR products were amplified from the same RNA samples and served as internal controls.

Cell line and RNAi. Human esophageal cancer-derived cell lines, TE1, TE3, TE5, TE7, and TE13, were kindly provided by Dr. Tetsuro Nishihara (Tohoku University School of Medicine, Miyagi, Japan).⁽¹⁹⁾ All cell lines were maintained in RPMI-1640 (Nissui Pharmaceutical, Tokyo, Japan) containing 10% FBS (Whittaker, Walkersville, MD, USA) in a humidified atmosphere of 5% CO₂ and 95% air at 37°C. To knockdown the endogenous *ADAMTS16*, RNAi was carried out. siRNA oligonucleotides for *ADAMTS16* and a negative control were purchased from Invitrogen (Carlsbad, CA, USA). Three independent oligonucleotides were used for *ADAMTS16* siRNA. The *ADAMTS16* siRNA1 sequence was 5'-CCA GUA UUA UCA CAU GGU CAC CAU U-3'. The *ADAMTS16* siRNA2

sequence was 5'-ACA GAG ACC UGA AGU UUC AAG UAA A-3'. The *ADAMTS16* siRNA3 sequence was 5'-GAG UAU AAG UCU UGC UUA CGG CAU A-3'. Transfection was carried out using Lipofectamine RNAiMAX (Invitrogen) according to the manufacturer's protocol. Briefly, 60 pmol siRNA and 10 µL Lipofectamine RNAiMAX were mixed in 1 mL RPMI medium (10 nmol/L final siRNA concentration). After 20 min of incubation, the mixture was added to the cells and these were plated on dishes for each assay. Forty-eight hours after transfection, cells were analyzed for all experiments.

Western blot analysis. For Western blot analysis, tissue samples or cells were lysed as described previously.⁽²⁰⁾ The culture media were concentrated with the Protein Concentrate Kit (Takara Bio, Shiga, Japan). The lysates (40 µg) were solubilized in Laemmli sample buffer by boiling, then subjected to 8% SDS-PAGE followed by electrotransfer onto a nitrocellulose filter. The filter was incubated with the primary antibody against *ADAMTS16* (rabbit polyclonal, dilution 1:500; Abcam, Cambridge, UK). Peroxidase-conjugated antirabbit IgG was used in the secondary reaction. Immunocomplexes were visualized with an ECL Western Blot Detection System (Amersham Biosciences). β-actin antibody (Sigma Chemical, St. Louis, MO, USA) was also used as a loading control.

Cell growth and in vitro invasion assays. The cells were seeded at a density of 2000 cells per well in 96-well plates. Cell growth was monitored after 1 and 2 days by MTT assay.⁽²¹⁾ Modified Boyden chamber assays were carried out to examine invasiveness. Cells were plated at 10 000 cells per well in RPMI-1640 medium plus 1% serum in the upper chamber of a Transwell insert (8 µm pore diameter; Chemicon, Temecula, CA, USA) coated with Matrigel. Medium containing 10% serum was added in the bottom chamber. After 1 and 2 days, cells in the upper chamber were removed by scraping, and the cells remaining on the lower surface of the insert were stained with CyQuant GR dye (Chemicon, Temecula, CA, USA) to assess the number of cells.

Statistical methods. Correlations between clinicopathologic parameters and *ADAMTS16* mRNA expression were analyzed by Fisher's exact test. A *P* value of <0.05 was considered statistically significant.

Results

Generation of SAGE data and comparison of expression patterns in ESCC and normal squamous esophagus. A total of 14 430 tags was generated, including 5765 that were unique. Then we compared SAGE tags from the ESCC sample with those from normal squamous esophagus (Gene Expression Omnibus accession number, GSM52501), which contained a total of 50 508 tags including 14 835 unique tags. The 20 most upregulated tags and the 20 most downregulated tags are shown in Tables 1 and 2. The upregulated tags included *ADAMTS16*, immunoglobulin heavy constant gamma 1 (*IGHG1*), 2-oxoglutarate and iron-dependent oxygenase domain containing 1 (*OGFOD1*), nuclear transport factor 2 (*NUTF2*), and RING1 and YY1 binding protein (*RYBP*), whose expressions have not been investigated in ESCC. The downregulated tags included S100 calcium binding protein A9 (*S100A9*), keratin 4 (*KRT4*), cystatin B (*CSTB*), exportin 7 (*XPO7*), keratin 6C (*KRT6C*), and epithelial membrane protein 1 (*EMP1*). Downregulation of some of these genes has been reported previously.⁽¹³⁾ To identify novel biomarkers for ESCC diagnosis and novel targets for ESCC treatment, we focused on genes that were upregulated in the ESCC sample. Of the upregulated genes, we decided to analyze *ADAMTS16* expression because the amino acid sequence of the *ADAMTS16* protein suggests that it might be secreted.

mRNA expression of *ADAMTS16*. Because genes expressed at high levels in tumors and at greatly reduced levels in normal tissues are ideal diagnostic markers and therapeutic targets,⁽⁴⁾

Table 1. Twenty most upregulated tags in esophageal squamous cell carcinoma (ESCC) compared to normal squamous esophagus (normal)

Tag sequence	Tags per million		Symbol	Description
	ESCC	Normal		
TCCCCTACAT	2564+ (37)†	0 (0)	<i>ADAMTS16</i>	ADAM metalloproteinase with thrombospondin type 1 motif, 16
GAAATAAAGC	2495 (36)	0 (0)	<i>IGHG1</i>	Immunoglobulin heavy constant gamma 1 (G1m marker)
TTCCGGTTGGT	2148 (31)	0 (0)	<i>OGFOD1</i>	2-Oxoglutarate and iron-dependent oxygenase domain containing 1
AGGCATTGAA	5336 (77)	20 (1)	<i>NUTF2</i>	Nuclear transport factor 2
CAGTTACAAA	5544 (80)	40 (2)	<i>RYBP</i>	RING1 and YY1 binding protein
TGGAAATGAC	1317 (19)	0 (0)	<i>COL1A1</i>	Collagen, type I, alpha 1
GGCGTTTAGA	2079 (30)	20 (1)	No match	No match
ACCAAAAACC	1663 (24)	20 (1)	<i>COL1A1</i>	Collagen, type I, alpha 1
GGCAGCACAA	1455 (21)	20 (1)	<i>NBEAL2</i>	Neurobeachin-like 2
TTTATTAGAA	1455 (21)	20 (1)	<i>CCDC75</i>	Coiled-coil domain containing 75
AGCCAAAAAA	2980 (43)	40 (2)	<i>MAP3K12</i>	Mitogen-activated protein kinase kinase kinase 12
GCTTTCATTG	2495 (36)	40 (2)	<i>NUCK5</i>	Nuclear casein kinase and cyclin-dependent kinase substrate 1
			<i>GPX2</i>	Glutathione peroxidase 2 (gastrointestinal)
ATGTGAAGAG	901 (13)	0 (0)	<i>SPARC</i>	Secreted protein, acidic, cysteine-rich (osteonectin)
CTCCCCAAA	693 (10)	0 (0)	<i>KLK10</i>	Kallikrein-related peptidase 10
			<i>IGHA2</i>	Immunoglobulin heavy constant alpha 2 (A2m marker)
GCTTAAAAAA	693 (10)	0 (0)	<i>CORO1C</i>	Coronin, actin binding protein, 1C
ATTGAGAGT	624 (9)	0 (0)	<i>MYH9</i>	Myosin, heavy chain 9, non-muscle
CTTTATTCCA	624 (9)	0 (0)	<i>WWC2</i>	WW and C2 domain containing 2
TCAAGCCATC	624 (9)	0 (0)	<i>BLMH</i>	Bleomycin hydrolase
			<i>PCYT2</i>	Phosphate cytidylyltransferase 2, ethanolamine
TTTTCAATT	624 (9)	0 (0)	<i>UTP3</i>	UTP3, small subunit (SSU) processome component, homolog (<i>S. cerevisiae</i>)
TTGCTACAAA	1178 (17)	20 (1)	<i>ABHD12B</i>	Abhydrolase domain containing 12B

†Absolute tag counts are normalized to 1 000 000 total tags/sample. ‡Number in parentheses indicates the absolute tag counts.

Table 2. Twenty most downregulated tags in esophageal squamous cell carcinoma (ESCC) compared to normal squamous esophagus (normal)

Tag sequence	Tags per million		Symbol	Description
	ESCC	Normal		
GTGGCCACGG	0 (0)	25 283+ (1277)†	<i>S100A9</i>	S100 calcium binding protein A9 (calgranulin B)
GGCAGAGAAG	0 (0)	8454 (427)	<i>KRT4</i>	Keratin 4
ATGAGCTGAC	0 (0)	3762 (190)	<i>CTSB</i>	Cystatin B (stefin B)
			<i>XPO7</i>	Exportin 7
GAAGCACAAAG	0 (0)	2475 (125)	<i>KRT6C</i>	Keratin 6C
TAATTTGCAT	0 (0)	2455 (124)	<i>EMP1</i>	Epithelial membrane protein 1
			<i>GNA13</i>	Guanine nucleotide binding protein (G protein), alpha 13
AAAGCGGGGC	0 (0)	2356 (119)	<i>KRT13</i>	Keratin 13
TGTGTTGAGA	0 (0)	2257 (114)	<i>EEF1A1</i>	Eukaryotic translation elongation factor 1 alpha 1
CACAAACGGT	0 (0)	2079 (105)	<i>TSPAN9</i>	Tetraspanin 9
			<i>RPS27</i>	Ribosomal protein S27
TGGTGTGAG	0 (0)	1841 (93)	<i>RPS18</i>	Ribosomal protein S18
GCCAATCCAG	0 (0)	1802 (91)	<i>CRNN</i>	Cornulin
GGCAAGCCCC	0 (0)	1782 (90)	<i>RPL10A</i>	Ribosomal protein L10a
			<i>PTPRG</i>	Protein tyrosine phosphatase, receptor type, G
AAGGAGATGG	0 (0)	1722 (87)	<i>RPL31</i>	Ribosomal protein L31
			<i>ZNF434</i>	Zinc finger protein 434
CTGTCACCCT	0 (0)	1564 (79)	<i>SPRR1A</i>	Small proline-rich protein 1A
			<i>BTC</i>	Betacellulin
TAAGGAGCTG	0 (0)	1485 (75)	<i>RPS26</i>	Ribosomal protein S26
			<i>ANK2</i>	Ankyrin 2, neuronal
ACCTGGAGGG	0 (0)	1386 (70)	<i>SBSN</i>	Suprabasin
			<i>PCBP1</i>	Poly(rC) binding protein 1
ACGTGTGTAA	0 (0)	1386 (70)	No match	No match
CAAATCCAAA	0 (0)	1366 (69)	No match	No match
GCCGAGGAAG	0 (0)	1346 (68)	<i>RPS12</i>	Ribosomal protein S12
			<i>NCKAP5L</i>	NCK-associated protein 5-like
TGTGCTAAAT	0 (0)	1346 (68)	<i>USP36</i>	Ubiquitin specific peptidase 36
			<i>RPL34</i>	Ribosomal protein L34
GGGTCTGAGG	0 (0)	1307 (66)	<i>SLURP1</i>	Secreted LY6/PLAUR domain containing 1
			<i>PTPRG</i>	Protein tyrosine phosphatase, receptor type, G

†The absolute tag counts are normalized to 1 000 000 total tags/sample. ‡Number in parentheses indicates the absolute tag counts.

quantitative RT-PCR of *ADAMTS16* was carried out in 20 ESCC samples and in 15 kinds of normal tissue (liver, kidney, heart, colon, brain, bone marrow, skeletal muscle, lung, small intestine, spleen, spinal cord, stomach, pancreas, leukocyte, and esophagus) (Fig. 2a). Among the various normal tissues, obvious *ADAMTS16* expression was found in normal brain, spinal cord, pancreas, and kidney, as reported elsewhere.⁽²²⁾ Expression of *ADAMTS16* in these normal tissues was highest in spinal cord; however, in ESCC, high levels of *ADAMTS16* mRNA expression (more than twice the mRNA expression of spinal cord) were found in eight out of 20 cases (40%). *ADAMTS16* expression in two ESCC cases (Cases 16 and 17) was 10-fold higher than in spinal cord. High levels of *ADAMTS16* mRNA expression were not correlated with any clinicopathologic characters (data not shown). Among five cases at stage I ESCC, a high level of *ADAMTS16* mRNA was detected in one case (20%). These results indicate that *ADAMTS16* expression is highly specific for cancer, at least in ESCC.

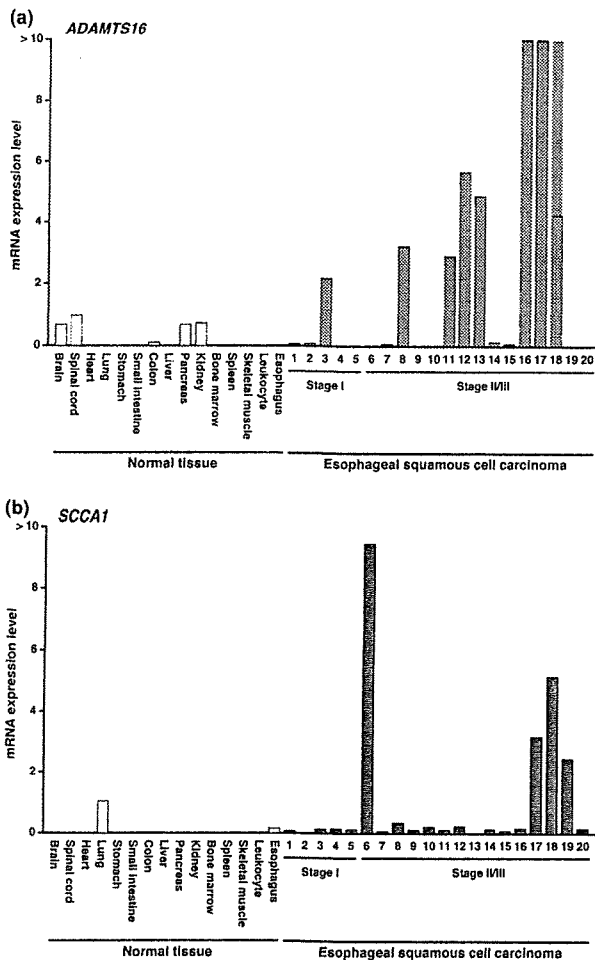


Fig. 2. Quantitative RT-PCR analysis of *ADAMTS16* and *SCCA1* in 15 kinds of normal tissues and 20 esophageal squamous cell carcinoma tissues. (a) mRNA expression level of *ADAMTS16*. The units are arbitrary, and we calculated *ADAMTS16* mRNA expression by standardization of the expression in normal spinal cord to 1.0. (b) mRNA expression level of *SCCA1*. The units are arbitrary, and we calculated *SCCA1* mRNA expression by standardization of the expression in normal lung to 1.0.

Serum squamous cell carcinoma antigen (SCC antigen) detected in the normal squamous epithelium and in ESCC has been considered a useful tumor marker for ESCC.⁽²³⁾ SCC antigen predicts recurrence or progression of the disease and has been used extensively for this purpose. However, clinical use of this marker has been restricted because of lack of sensitivity.⁽²⁴⁾ Therefore, there is an urgent need for new biomarkers for ESCC. To evaluate the usefulness of determining *ADAMTS16* expression as a tumor marker, we measured expression levels of SCC antigen and compared them with *ADAMTS16* levels. Because a measurement system for serum levels of *ADAMTS16* is not available, we investigated the mRNA expression levels of *SCCA1*, which encodes SCC antigen, by quantitative RT-PCR (Fig. 2b). In 15 kinds of normal tissue, expression of *SCCA1* was highest in lung; however, in ESCC, high levels of *SCCA1* mRNA expression (more than twice the mRNA expression levels of lung) were found in four of 20 cases (20%). Among five cases at stage I ESCC, high levels of *SCCA1* mRNA were not detected. These results indicate that *ADAMTS16* might serve as a more sensitive biomarker than SCC antigen. We calculated the ratio of *ADAMTS16* mRNA expression levels between ESCC tissue (T) and corresponding non-neoplastic mucosa (N). T/N ratios >2-fold higher were considered to represent overexpression. *ADAMTS16* overexpression was observed in 13 of 20 ESCC cases (65%). Among five cases at stage I ESCC, *ADAMTS16* overexpression was found in one case (20%). We then investigated the relation of *ADAMTS16* expression to clinicopathologic characters (Table 3). We found that *ADAMTS16* overexpression correlated to the advanced T classification and tumor stage.

ADAMTS16 protein expression. Analysis of the amino acid sequence of the *ADAMTS16* protein suggests that it might be secreted. To investigate whether *ADAMTS16* is a secreted protein, we used Western blot analysis in five esophageal cancer cell lines. Moderate to high *ADAMTS16* expression was noted in TE1, TE3, and TE5 cells as a band of approximately 136 kDa, and the other two remaining cell lines (TE7 and TE13) had low or absent *ADAMTS16* expression (Fig. 3a). Next, we examined the transition of *ADAMTS16* expression by Western blot analysis of cell extracts of TE5 transfected with *ADAMTS16* specific siRNAs. Three types of siRNAs (siRNA1-3) were transfected into TE5. The expression of *ADAMTS16* in TE5 was substantially suppressed by treatment with siRNA2

Table 3. Relationship between *ADAMTS16* expression and clinicopathologic characteristics in esophageal squamous cell carcinoma

	<i>ADAMTS16</i> expression		P value*
	Overexpression	No overexpression	
Age (years)			
≤65	8 (80%)	2 (20%)	0.3498
>65	5 (50%)	5 (50%)	
Sex			
Male	11 (69%)	5 (31%)	0.5868
Female	2 (50%)	2 (50%)	
T classification			
T1	2 (29%)	5 (71%)	0.0215
T2/3	11 (85%)	2 (15%)	
N classification			
N0	3 (43%)	4 (57%)	0.1736
N1	10 (77%)	3 (23%)	
Stage			
Stage I	1 (20%)	4 (80%)	0.0307
Stage II/III	12 (80%)	3 (20%)	

*Fisher's exact test. N, node; T, tumor.

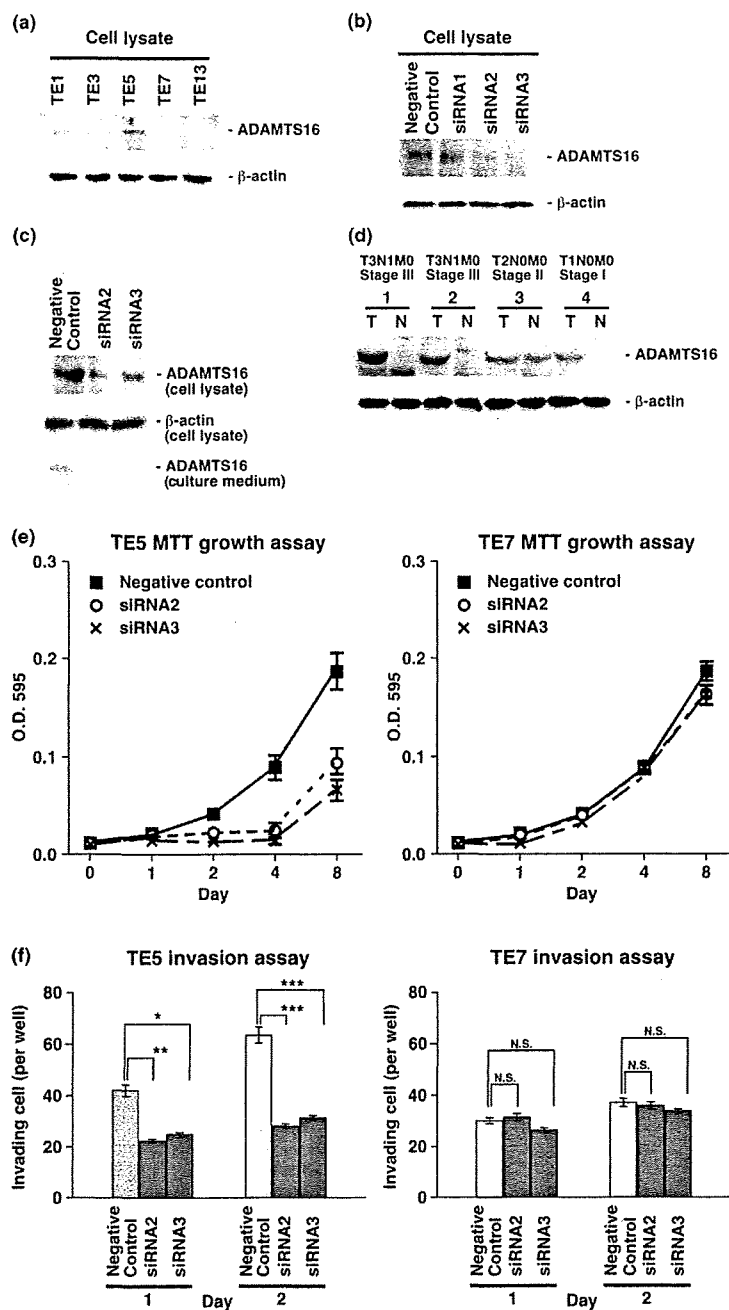


Fig. 3. ADAMTS16 protein expression and functional analysis. (a) Western blot analysis of ADAMTS16 in five esophageal squamous cell carcinoma (ESCC) cell lines. (b) Western blot analysis of ADAMTS16 in cell lysates from TE5 cells transfected with the negative control siRNA and ADAMTS16 siRNA (siRNA1–3). (c) Western blot analysis of ADAMTS16 in cell lysates and culture media from TE5 cells transfected with the negative control siRNA and ADAMTS16 siRNA (siRNA2 and 3). (d) Western blot analysis of ADAMTS16 in four ESCC samples (T) and corresponding non-neoplastic mucosa samples (N). (e) Effect of ADAMTS16 knockdown on cell growth of TE5 and TE7 cells. Cell growth was assessed by an MTT assay at 1, 2, 4, and 8 days after seeding on 96-well plates. Bars and error bars, mean and SE of three different experiments. O.D., optical density. (f) Effect of ADAMTS16 knockdown on cell invasion of TE5 and TE7 cells. TE5 and TE7 cells transfected with negative control siRNA and ADAMTS16 siRNA (siRNA2 and 3) were incubated in Boyden chambers. After 1 and 2 days, invading cells were counted. Bars and error bars, mean and SE of three different experiments. N.S., not significant. * $P = 0.0006$; ** $P = 0.0003$; *** $P < 0.0001$.

and siRNA3, but not with siRNA1 (Fig. 3b). Therefore, to knock down the endogenous ADAMTS16, we used siRNA2 and siRNA3 in the following experiments. A Western blot was car-

ried out of siRNA (siRNA2 and siRNA3)-transfected TE5 cell extracts and culture media (Fig. 3c). In negative control siRNA-transfected TE5 cells, ADAMTS16 protein was detected in

culture media as well as cell extracts; however, in ADAMTS16 siRNA-transfected TE5 cells, ADAMTS16 protein was low or absent in culture media as well as cell extracts. These results clearly indicate that ADAMTS16 is a secreted protein.

Next, expression of ADAMTS16 protein was analyzed by a Western blot of four ESCC tissue samples and corresponding non-neoplastic mucosa samples (Fig. 3d). Among the four ESCC samples, ADAMTS16 protein expression was detected in all; however, of the four corresponding non-neoplastic mucosa samples, ADAMTS16 protein expression was found in only one sample. These results indicate that ADAMTS16 protein is overexpressed in ESCC tissue, and can serve as a serum tumor marker for ESCC.

Effect of ADAMTS16 inhibition on cell growth and invasive activity of esophageal cancer cells. High levels of *ADAMTS16* mRNA expression were correlated with T classification of ESCC tissues; however, the biological significance of ADAMTS16 in ESCC has not been studied. To investigate the possible antiproliferative effects of ADAMTS16 knockdown, we carried out an MTT assay 8 days after siRNA transfection (Fig. 3e). TE5 cells were selected for high ADAMTS16 expression. ADAMTS16 siRNA2-transfected and siRNA3-transfected TE5 cells showed significantly reduced viability relative to negative control siRNA-transfected TE5 cells. We carried out the same assay using one additional esophageal cancer cell line that did not express ADAMTS16 (TE7). Reduced cell viability was not observed in siRNA2- or siRNA3-transfected TE7 cells compared with negative control siRNA-transfected TE7 cells.

Next, to determine the possible role of ADAMTS16 in the invasiveness of esophageal cancer cells, we used a Transwell invasion assay (Fig. 3f). On day 1, although there was no difference in cell viability between ADAMTS16 knockdown TE5 cells and negative control siRNA-transfected TE5 cells, the invasiveness of ADAMTS16 knockdown TE5 cells was 40% less than that of the negative control siRNA-transfected TE5 cells. On day 2, the invasiveness of ADAMTS16 knockdown TE5 cells was 50% less than that of the negative control siRNA-transfected TE5 cells; however, as ADAMTS16 knockdown cells showed significantly reduced cell viability, the cell number difference observed in the invasion assay might be caused by the reduced cell viability. In contrast, invasion ability was not significantly different between ADAMTS16 knockdown TE7 cells and negative control siRNA-transfected TE7 cells. These results indicate that ADAMTS16 stimulates cell growth and invasion in esophageal cancer cells.

Discussion

In spite of improvement to modern surgical techniques and adjuvant CRT, ESCC is known to reveal the worst prognosis among malignant tumors. Therefore, it is now urgently required to develop novel diagnostic biomarkers and therapeutic targets for a better choice of adjuvant treatment modalities for individual patients. In the present study, we carried out a genome-wide expression profile analysis of one ESCC tissue sample by SAGE, and identified upregulated and downregulated genes in ESCC. Among these, we further investigated *ADAMTS16*. Quantitative RT-PCR revealed that *ADAMTS16* mRNA expression was frequently upregulated in ESCC, and was narrowly restricted in normal tissues. Western blot analysis also showed upregulation of ADAMTS16 protein in ESCC. Furthermore, ADAMTS16 protein was detected in culture media from TE5 cells. Taken together, these results suggest that ADAMTS16 has potential as a serum tumor marker for ESCC. Because the frequency of high levels of *ADAMTS16* mRNA expression (40%) was greater than the frequency of high levels of *SCCA1* mRNA expression (20%), serum concentrations of ADAMTS16 might

serve as a sensitive biomarker for ESCC. In contrast, because *ADAMTS16* mRNA overexpression was correlated with advanced T classification and tumor stage, serum concentrations of ADAMTS16 might not be suitable for early detection of ESCC. Serum concentrations of ADAMTS16 should be measured in patients with ESCC.

In the present study, *ADAMTS16* mRNA overexpression correlated to the advanced T classification and tumor stage. Knockdown of ADAMTS16 by RNAi inhibited the cell growth and invasion ability of TE5 cells. Because expression of ADAMTS16 was highly specific to ESCC, it could be a good therapeutic target with less adverse effects for ESCC. Although the function of ADAMTS16 is poorly understood, members of the metzincin family are known to process a number of growth factors, cytokines and signaling molecules in addition to matrix substrates.⁽²⁵⁾ However, it has been reported that the forced expression of ADAMTS16 has no effect on expression levels of most of the ADAMTS, TIMP, and MMP genes. In the present study, we also used ELISA to measure levels of epidermal growth factor (EGF) and transforming growth factor (TGF)- α in culture media from TE5 cells transfected with ADAMTS16 siRNA and negative control siRNA; however, levels of EGF and TGF- α were not significantly different (data not shown). Therefore, growth factors or cytokines, such as EGF or TGF- α , are not likely to be involved in mechanisms of cell growth inhibition and invasion ability following knockdown of ADAMTS16.

Although ADAMTS16 protein upregulation was observed in ESCC tissues by Western blot analysis, expression and distribution of ADAMTS16 protein in ESCC tissues remains unclear. Therefore, immunohistochemical analysis should be undertaken. Unfortunately, the antibody against ADAMTS16 used in the present study is not suitable for immunostaining because the antibody against ADAMTS16 detected multiple bands on Western blots. Production of a specific antibody against ADAMTS16 is required. Furthermore, ADAMTS16 expression at mRNA and protein levels should be examined in several more tissues from stage I ESCC in the near future.

In addition to *ADAMTS16*, other upregulated and downregulated genes in ESCC were found. The upregulated group of genes identified by SAGE contains genes whose expression has not been investigated in ESCC. Upregulation of two genes related to the immunoglobulin heavy chain (*IGHG1* and *IGHA2*) was found in the present study. Previously, genes involved in the immune response have been shown as characteristically upregulated in long-term ESCC survivors who were treated with CRT.⁽²⁶⁾ Therefore, the ESCC case analyzed by SAGE in the present study might be sensitive to CRT. *OGFOD1* is a 2-oxoglutarate and Fe(II)-dependent oxygenase, a class of enzymes that catalyze a variety of reactions typically involving the oxidation of an organic substrate using a dioxygen molecule.⁽²⁷⁾ To our knowledge, association between cancer and *OGFOD1* has not been investigated. *NUTF2* encodes nuclear transport factor 2 (NTF2), which is a small GDP Ran binding protein. The main function of NTF2 is to facilitate transport of certain proteins into the nucleus through interaction with nucleoporin FxFG.⁽²⁸⁾ It is also involved in regulating multiple processes, including cell cycle and apoptosis.⁽²⁹⁾ However, no studies have analyzed NTF2 expression in human cancer, including ESCC. *RYBP* is a member of the polycomb group, and it has been reported that RYBP interacts with MDM2 and decreases MDM2-mediated p53 ubiquitination, leading to stabilization of p53 and an increase in p53 activity.⁽³⁰⁾ RYBP induces cell cycle arrest and is involved in the p53 response to DNA damage. Expression of RYBP is decreased in hepatocellular carcinoma and lung cancer tissues.⁽³⁰⁾ Therefore, upregulation of RYBP should be confirmed in a large number of ESCC cases. In contrast, downregulated genes identified by SAGE in the present study were

similar to genes previously reported as downregulated in ESCC.⁽¹³⁾

In conclusion, our present SAGE data provide a list of genes potentially associated with ESCC. Because our list is based on one ESCC case, expression analysis in a large number of cases is required. A high level of *ADAMTS16* expression was detected in ESCC, and expression of *ADAMTS16* was narrowly restricted. Production of a specific antibody against *ADAMTS16* protein and establishment of a measurement system for serum samples are needed to clarify whether *ADAMTS16* serves as a serum marker for early detection and a good therapeutic target for ESCC.

References

- 1 Enzinger PC, Mayer RJ. Esophageal cancer. *N Engl J Med* 2003; **349**: 2241–52.
- 2 Goseki N, Koike M, Yoshida M. Histopathologic characteristics of early stage esophageal carcinoma. A comparative study with gastric carcinoma. *Cancer* 1992; **69**: 1088–93.
- 3 Tamoto E, Tada M, Murakawa K *et al*. Gene-expression profile changes correlated with tumor progression and lymph node metastasis in esophageal cancer. *Clin Cancer Res* 2004; **10**: 3629–38.
- 4 Buckhaults P, Rago C, St Croix B *et al*. Secreted and cell surface genes expressed in benign and malignant colorectal tumors. *Cancer Res* 2001; **61**: 6996–7001.
- 5 Yasui W, Oue N, Ito R, Kuraoka K, Nakayama H. Search for new biomarkers of gastric cancer through serial analysis of gene expression and its clinical implications. *Cancer Sci* 2004; **95**: 385–92.
- 6 Lu J, Liu Z, Xiong M *et al*. Gene expression profile changes in initiation and progression of squamous cell carcinoma of esophagus. *Int J Cancer* 2001; **91**: 288–94.
- 7 Kan T, Shimada Y, Sato F *et al*. Prediction of lymph node metastasis with use of artificial neural networks based on gene expression profiles in esophageal squamous cell carcinoma. *Ann Surg Oncol* 2004; **11**: 1070–8.
- 8 Velculescu VE, Zhang L, Vogelstein B, Kinzler KW. Serial analysis of gene expression. *Science* 1995; **270**: 484–7.
- 9 Oue N, Hamai Y, Mitani Y *et al*. Gene expression profile of gastric carcinoma: identification of genes and tags potentially involved in invasion, metastasis, and carcinogenesis by serial analysis of gene expression. *Cancer Res* 2004; **64**: 2397–405.
- 10 Aung PP, Oue N, Mitani Y *et al*. Systematic search for gastric cancer-specific genes based on SAGE data: melanoma inhibitory activity and matrix metalloproteinase-10 are novel prognostic factors in patients with gastric cancer. *Oncogene* 2006; **25**: 2546–57.
- 11 Mitani Y, Oue N, Matsumura S *et al*. Reg IV is a serum biomarker for gastric cancer patients and predicts response to 5-fluorouracil-based chemotherapy. *Oncogene* 2007; **26**: 4383–93.
- 12 Oue N, Sentani K, Noguchi T *et al*. Serum olfactomedin 4 (GW112, hGC-1) in combination with Reg IV is a highly sensitive biomarker for gastric cancer patients. *Int J Cancer* 2009; **125**: 2383–92.
- 13 van Baal JW, Milana F, Rygiel AM *et al*. A comparative analysis by SAGE of gene expression profiles of esophageal adenocarcinoma and esophageal squamous cell carcinoma. *Cell Oncol* 2008; **30**: 63–75.
- 14 van Baal JW, Milano F, Rygiel AM *et al*. A comparative analysis by SAGE of gene expression profiles of Barrett's esophagus, normal squamous esophagus, and gastric cardia. *Gastroenterology* 2005; **129**: 1274–81.
- 15 Mochizuki S, Okada Y. ADAMs in cancer cell proliferation and progression. *Cancer Sci* 2007; **98**: 621–8.
- 16 Rodriguez-Lopez J, Pombou-Suarez M, Loughlin J *et al*. Association of a nsSNP in *ADAMTS14* to some osteoarthritis phenotypes. *Osteoarthritis Cartilage* 2009; **17**: 321–7.
- 17 Sobin LH, Wittekind CH, eds. *TNM Classification of Malignant Tumors*, 6th edn. New York: Wiley-Liss, 2002; 60–4.
- 18 Kondo T, Oue N, Yoshida K *et al*. Expression of POT1 is associated with tumor stage and telomere length in gastric carcinoma. *Cancer Res* 2004; **64**: 523–9.
- 19 Nishihira T, Hashimoto Y, Katayama M, Mori S, Kuroki T. Molecular and cellular features of esophageal cancer cells. *J Cancer Res Clin Oncol* 1993; **119**: 441–9.
- 20 Yasui W, Sano T, Nishimura K *et al*. Expression of P-cadherin in gastric carcinomas and its reduction in tumor progression. *Int J Cancer* 1993; **54**: 49–52.
- 21 Alley MC, Scudiero DA, Monks A *et al*. Feasibility of drug screening with panels of human tumor cell lines using a microculture tetrazolium assay. *Cancer Res* 1988; **48**: 589–601.
- 22 Cal S, Obaya AJ, Llamazares M, Garabaya C, Quesada V, Lopez-Otin C. Cloning, expression analysis, and structural characterization of seven novel human *ADAMTSs*, a family of metalloproteinases with disintegrin and thrombospondin-1 domains. *Gene* 2002; **283**: 49–62.
- 23 Mino-Miyagawa N, Kimura Y, Hamamoto K. Tumor-antigen 4. Its immunohistochemical distribution and tissue and serum concentrations in squamous cell carcinoma of the lung and esophagus. *Cancer* 1990; **66**: 1505–12.
- 24 Sugimachi K, Kitamura M, Matsuda H, Okudaira Y. Tumor antigen TA-4: an aid in detecting post-operative recurrences of esophageal carcinoma. *Dis Markers* 1987; **5**: 67–73.
- 25 Somerville RP, Oblander SA, Apte SS. Matrix metalloproteinases: old dogs with new tricks. *Genome Biol* 2003; **4**: 216.
- 26 Ashida A, Boku N, Aoyagi K *et al*. Expression profiling of esophageal squamous cell carcinoma patients treated with definitive chemoradiotherapy: clinical implications. *Int J Oncol* 2006; **28**: 1345–52.
- 27 Aravind L, Koonin EV. The DNA-repair protein AlkB, EGL-9, and leprecan define new families of 2-oxoglutarate- and iron-dependent dioxygenases. *Genome Biol* 2001; **2**: 1–8.
- 28 Isgro TA, Schulten K. Association of nuclear pore FG-repeat domains to NTF2 import and export complexes. *J Mol Biol* 2007; **366**: 330–45.
- 29 Makhnevych T, Lusk CP, Anderson AM, Aitchison JD, Wozniak RW. Cell cycle regulated transport controlled by alterations in the nuclear pore complex. *Cell* 2003; **115**: 813–23.
- 30 Chen D, Zhang J, Li M, Rayburn ER, Wang H, Zhang R. RYBP stabilizes p53 by modulating MDM2. *EMBO Rep* 2009; **10**: 166–72.

Acknowledgment

We thank Mr. Shinichi Norimura for excellent technical assistance and advice. We thank the Analysis Center of Life Science, Hiroshima University (Hiroshima, Japan) for the use of their facilities. This work was supported, in part, by Grants-in-Aid for Cancer Research from the Ministry of Education, Culture, Science, Sports, and Technology of Japan, partly by a Grant-in-Aid for the Third Comprehensive 10-Year Strategy for Cancer Control and for Cancer Research from the Ministry of Health, Labour, and Welfare of Japan, and partly by a grant (07-23911) from the Princess Takamatsu Cancer Research Fund.

ORIGINAL ARTICLE

Wnt5a signaling is involved in the aggressiveness of prostate cancer and expression of metalloproteinase

H Yamamoto^{1,2}, N Oue³, A Sato⁴, Y Hasegawa⁵, H Yamamoto⁴, A Matsubara⁵, W Yasui³ and A Kikuchi⁴

¹Department of Biochemistry, Graduate School of Biomedical Sciences, Hiroshima University, Hiroshima, Japan; ²Department of Surgery, Graduate School of Biomedical Sciences, Hiroshima University, Hiroshima, Japan; ³Department of Molecular Pathology, Graduate School of Biomedical Sciences, Hiroshima University, Hiroshima, Japan; ⁴Department of Molecular Biology and Biochemistry, Graduate School of Medicine, Faculty of Medicine, Osaka University, Suita, Japan and ⁵Department of Urology, Graduate School of Biomedical Sciences, Hiroshima University, Hiroshima, Japan

Wnt5a is a representative ligand that activates the β -catenin-independent pathway in Wnt signaling. Although it has been reported that abnormal activation of the Wnt/ β -catenin-dependent pathway is often observed in human prostate cancer, the involvement of the β -catenin-independent pathway in this cancer is unclear. Abnormal expression of Wnt5a and β -catenin was observed in 27 (28%) and 49 (50%) of 98 prostate cancer cases, respectively, by immunohistochemical analyses. Simultaneous expression of Wnt5a and β -catenin was observed in only five cases, suggesting their exclusive expression. The positive detection of Wnt5a was correlated with high Gleason scores and biochemical relapse of prostate cancer, but that of β -catenin was not. Knockdown and overexpression of Wnt5a in human prostate cancer cell lines reduced and stimulated, respectively, their invasion activities, and the invasion activity required Frizzled2 and Ror2 as Wnt receptors. Wnt5a activated Jun-N-terminal kinase through protein kinase D (PKD) and the inhibition of PKD suppressed Wnt5a-dependent cell migration and invasion. In addition, Wnt5a induced the expression of metalloproteinase-1 through the recruitment of JunD to its promoter region. These results suggest that Wnt5a promotes the aggressiveness of prostate cancer and that its expression is involved in relapse after prostatectomy.

Oncogene advance online publication, 18 January 2010; doi:10.1038/onc.2009.496

Keywords: Wnt5a; prostate cancer; Gleason score; invasion; MMP-1

Introduction

Prostate cancer (PCa) is an increasingly prevalent cancer in men, which develops and progresses under the

influence of androgenic steroids (Jemal *et al.*, 2008). PCa screening by assessing serum prostate-specific antigen (PSA) level has led to increased detection of early-stage PCa that can be cured by radical prostatectomy or radiation therapy. Although overall cancer control rates are high for clinically localized diseases, 20–30% of patients will experience recurrence manifested initially as a rising PSA level without clinical or radiographic metastasis (Han *et al.*, 2003). This biochemical relapse is indicative of the presence of prostate tissue and is assumed to represent cancer. Many patients with biochemical relapse have indolent disease that grows slowly and requires no treatment but some will have rapid progression. A critical issue for patients is determination of whether rising PSA represents local or systemic disease, as the former may be cured by salvage radiotherapy and the latter requires hormone therapy. High risk of recurrence is defined according to preoperative PSA level (>20 ng/ml), biopsy Gleason score (≥ 8) and the 1992 American Joint Committee on Cancer clinical T stage ($\geq T2c$) (Partin *et al.*, 1997; D'Amico *et al.*, 2000). These factors are helpful but not perfect due to significant clinical heterogeneity. Identifying molecules that are expressed in clinically localized PCa but associated with PCa invasion and metastasis might significantly improve the prognostic capabilities and management of patients with PCa after a curative approach.

The accumulation of cytoplasmic and nuclear β -catenin has been documented in many malignancies, including breast, gastric, colon, esophageal, hepatic, pancreatic, thyroid, cerebellar and skin carcinoma (Polakis, 2000; Kikuchi, 2003). In PCa, abnormal accumulation of β -catenin has been detected in 20–50% of tumors, and high levels of β -catenin expression are associated with advanced, metastatic and hormone-refractory PCa (Yardy and Brewster, 2005). Although β -catenin was originally identified as a cadherin-binding protein, it is known to be a key molecule in the Wnt signaling pathway. Wnt proteins are a large family of cysteine-rich secreted molecules that exhibit unique expression patterns and distinct functions in development (Logan and Nusse, 2004). The well-established intracellular signaling pathway activated by Wnt proteins is a β -catenin-dependent signaling pathway that is

Correspondence: Dr A Kikuchi, Department of Molecular Biology and Biochemistry, Graduate School of Medicine, Faculty of Medicine, Osaka University, 2-2, Yamadaoka, Suita 565-0871, Japan.
E-mail: akikuchi@molbiobc.med.osaka-u.ac.jp
Received 4 August 2009; revised 4 November 2009; accepted 8 December 2009

highly conserved among species (Logan and Nusse, 2004; Kikuchi *et al.*, 2009). When Wnt acts on its cell-surface receptor, which consists of Frizzled and low-density lipoprotein receptor-related protein 5/6, cytoplasmic β -catenin is stabilized by release from the Axin complex. The accumulated β -catenin is translocated to the nucleus, where it binds to the transcription factor T-cell factor/lymphoid enhancer factor and thereby stimulates the expression of various genes (Hurlstone and Clevers, 2002). At least 19 Wnt members have been shown to be present in mammals to date, and some Wnts, including Wnt1, Wnt3a and Wnt7a, activate the β -catenin pathway. In addition to T-cell factor/lymphoid enhancer factor, β -catenin binds to androgen receptor, and these Wnt ligands also increase androgen receptor-mediated transcription even in the absence of androgen ligands (Verras *et al.*, 2004). Therefore, activation of the β -catenin pathway appears to be involved in the initiation and progression of PCa as shown in other tumors.

Another class of Wnts, including Wnt2, Wnt4, Wnt5a, Wnt5b, Wnt6 and Wnt11, activates a β -catenin-independent pathway that primarily modulates cell movement and polarity (Veeman *et al.*, 2003). This pathway is known to activate several protein kinases including Ca^{2+} /calmodulin-dependent protein kinase II, protein kinase C (PKC), c-jun N-terminal kinase (JNK) and Rho-associated kinase. Wnt5a is a representative of the Wnt proteins that activate the β -catenin-independent pathway, which includes multiple pathways, and Wnt5a activates distinct routes (Veeman *et al.*, 2003; Kurayoshi *et al.*, 2007; Kikuchi and Yamamoto, 2008). It has been shown that Wnt5a stimulates migration in some cancer cells and that its expression is correlated with the aggressiveness of melanoma, breast cancer, lung cancer and gastric cancer (Weeraratna *et al.*, 2002; Veeman *et al.*, 2003; Huang *et al.*, 2005; Kurayoshi *et al.*, 2006; Pukrop *et al.*, 2006; Kikuchi and Yamamoto, 2008; Yamamoto *et al.*, 2009), suggesting that Wnt5a has oncogenic properties. Other reports indicate that Wnt5a acts as a tumor suppressor based on the finding that Wnt5a has an ability to inhibit proliferation, migration and invasiveness in thyroid tumor and colorectal cancer cell lines (Dejmek *et al.*, 2005; Krementevskaja *et al.*, 2005). Although the β -catenin-independent pathway activated by Wnt5a is also involved in tumorigenesis, the relationship between the expression of Wnt5a and PCa is not well understood. This study showed that a high expression level of Wnt5a significantly correlates with biochemical relapse of clinically localized PCa cases treated with radical prostatectomy. It was also shown that Wnt5a promotes invasion activities of PCa cells at least through the activation of JNK and the expression of matrix metalloproteinase-1 (MMP-1).

Results

Immunohistochemical analysis of Wnt5a in PCa tissues

Preceding immunohistochemical studies showed that approximately 30% of 237 gastric cancer cases exhibit high expression levels of Wnt5a (Kurayoshi

et al., 2006). Using the same antibody, we examined the expression of Wnt5a in PCa. In adjacent non-neoplastic prostate tissue including glandular hyperplasia, weak or no staining of Wnt5a was observed in epithelial and stromal cells (Figure 1a). However, PCa tissue showed stronger and more extensive staining than corresponding non-neoplastic mucosa (Figure 1a). In the majority of PCa cases containing Wnt5a-positive tumor cells, more than 50% of the tumor cells showed cytoplasmic staining for Wnt5a. Of 98 PCa cases, 27 (28%) were positive for Wnt5a. In these PCa cases, no tendency of strong staining for Wnt5a at the invasive front was observed. The relationship between Wnt5a staining and clinicopathological characteristics was analyzed. Wnt5a positivity was found more frequently in PCa showing a Gleason score ≥ 8 (12/24, 50%) than in PCa showing a Gleason score ≤ 7 (15/74, 20%, $P=0.0079$, Fisher's exact test) (Supplementary Table S1). Therefore, the expression of Wnt5a may be associated with the aggressiveness of PCa. However, Wnt5a staining did not correlate with age, pT classification or preoperative PSA concentration (Supplementary Table S1).

An immunohistochemical analysis of β -catenin expression in PCa was also performed. Although β -catenin was usually detected at the cell membranes, cytosomal or nuclear accumulation of β -catenin was observed in 49 (50%) of 98 PCa cases (Supplementary Table S2). However, β -catenin staining in cytoplasm and nucleus did not correlate with age, pT classification, Gleason score or preoperative PSA concentration (Supplementary Table S2). These results suggested that the abnormal expression of β -catenin may be involved in the initiation of PCa but not in the aggressiveness of the tumor. The relationship between the expression of Wnt5a and β -catenin in PCa was analyzed further. Wnt5a positivity was found more frequently in cytosomal or nuclear β -catenin-negative cases (22/49, 45%) than in cytosomal or nuclear β -catenin-positive cases (5/49, 10%, $P=0.0002$, Fisher's exact test) (Supplementary Table S1). In the five PCa cases positive for both Wnt5a and cytosomal or nuclear β -catenin, there was a tendency that Wnt5a-positive cancer cells do not show cytosomal or nuclear accumulation of β -catenin (Figure 1b). These findings suggested that Wnt5a and cytosomal and nuclear β -catenin are expressed in an exclusive pattern in PCa.

Relapse of patients with PCa expressing Wnt5a

Next, the relationship between Wnt5a immunostaining and relapse in PCa was examined. Univariate analysis revealed that the expression of Wnt5a ($P=0.0045$, log-rank test) decreases the ratios of relapse-free survival in patients as well as high Gleason score ($P<0.0001$) and high preoperative PSA concentration ($P=0.0167$) (Figure 2a), whereas cytosomal or nuclear accumulation of β -catenin, age and pT classification did not correlate with relapse (Figure 2b). A Cox proportional hazards multivariate model was used to examine the relationship between clinicopathological factors, expression of Wnt5a and β -catenin, and relapse-free survival. Multi-

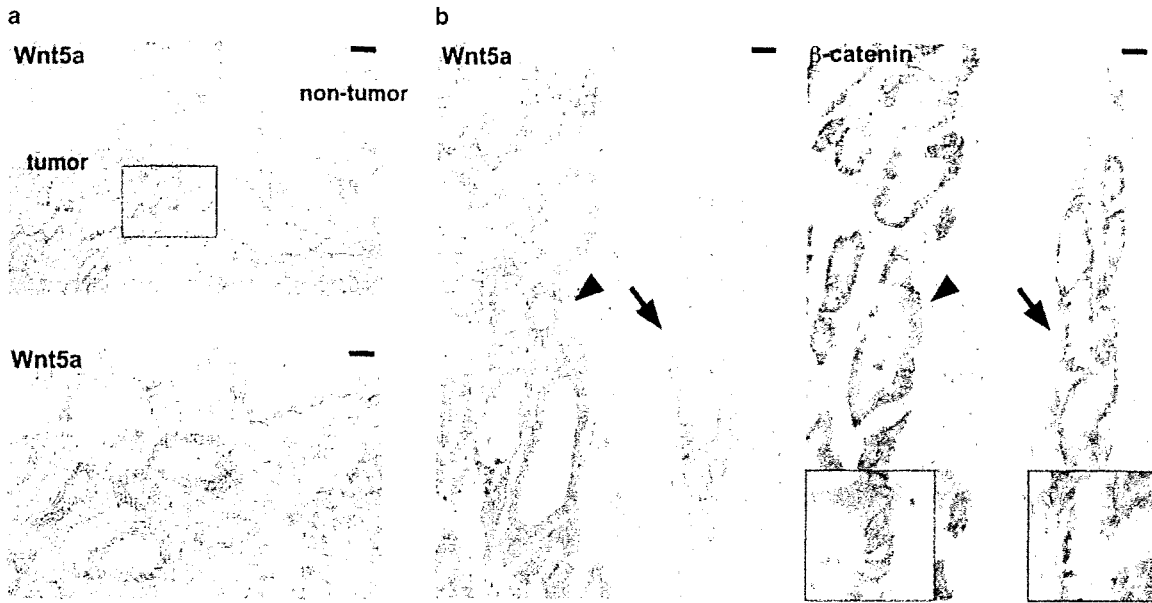


Figure 1 Immunohistochemical analyses of Wnt5a and β -catenin in prostate cancer (PCa). (a) Top panel, expression levels of Wnt5a in nontumor and tumor regions were compared. Bar, 50 μ m. Bottom panel, high-magnification image of the fields indicated by the box in the upper panel. The tumor regions were enlarged. Bar, 12 μ m. (b) A sample of PCa was stained with anti-Wnt5a (left panel) and anti- β -catenin (right panel) antibodies. Bars, 25 μ m. Arrowheads indicate Wnt5a-positive and cytosomal or nuclear β -catenin-negative PCa cells. Arrows indicate Wnt5a-negative and cytosomal or nuclear β -catenin-positive PCa cells. Insets, high-magnification images of the fields indicated by the arrow and arrowhead in the right panel.

variate analysis indicated that Wnt5a staining, Gleason score and preoperative PSA concentration are independent predictors of relapse of PCa, but cytosomal or nuclear β -catenin staining, age and pT classification are not (Table 1). These results suggested that Wnt5a expression contributes directly to the malignant potential of PCa.

Involvement of Wnt5a in migration and invasion of PCa cells

To understand the relationship between the expression of Wnt5a and aggressiveness of PCa, we examined the expression levels of various Wnts in PCa cells (Figure 3a). DU145 and PC3 cells are androgen-independent PCa cells and LNCap cells are androgen-dependent PCa cells. *Wnt5a* mRNA was highly expressed in DU145 and LNCap cells, but PC3 cells showed a low expression level. mRNA expression of *Wnt4* was observed in all cell lines. *Wnt5b* mRNA was detected in DU145 but not in LNCap and PC3 cells. Neither *Wnt3a* nor *Wnt11* mRNA was detected in these cells. Wnt5a siRNA reduced the mRNA level of *Wnt5a* in LNCap cells and suppressed migration activity in transwell assays using a Boyden chamber (Figure 3b, Supplementary Figure S1). Knockdown of Wnt5a in DU145 cells also decreased cell migration (Figure 3c), but knockdown of Wnt5b did not (data not shown). Wnt7a siRNA did not affect cell migration of LNCap and DU145 cells (Figures 3b and c, Supplementary Figure S1). Migration activity in Wnt4-knockdown cells

was decreased to about 70% of control cell (Figure 3c). Wnt4 has been reported to activate both the β -catenin-dependent and β -catenin-independent pathways (Bernard and Harley, 2007), but the role of Wnt4 in cell migration is not well understood. Therefore, we did not study the role of Wnt4 in migration of PCa cells further. It is known that DU145 and PC3 cells, but not LNCap cells, have invasion activities. Whereas control DU145 cells invaded the Matrigel, Wnt5a knockdown cells were less invasive (Figure 3c). Transient overexpression of Wnt5a enhanced the invasion activities of PC3 cells, but that of Wnt5a CA, which is an inactive form of Wnt5a generated by mutating Cys104 to Ala (Kurayoshi *et al.*, 2007), did not (Figure 3d).

Secreted Frizzled-related protein 2 (sFRP2) binds to Wnt proteins and acts as a negative regulator of Wnt signaling (Kawano and Kypta, 2003). DU145 cells were allowed to migrate in scratch-wound cultures, resulting in wound closure after 24 h, and the migration of DU145 cells in scratch-wound cultures was inhibited by the addition of sFRP2 conditioned medium (CM) (Figure 3e). Furthermore, an anti-Wnt5a antibody suppressed the migration of DU145 cells in scratch-wound cultures (Figure 3f). Taken together, these results indicated that Wnt5a stimulates cell migration and invasion in PCa cells.

Mechanism of Wnt5a-induced invasion by PCa cells

The mechanism by which Wnt5a induces invasion of DU145 and PC3 cells was examined as an *in vitro* model

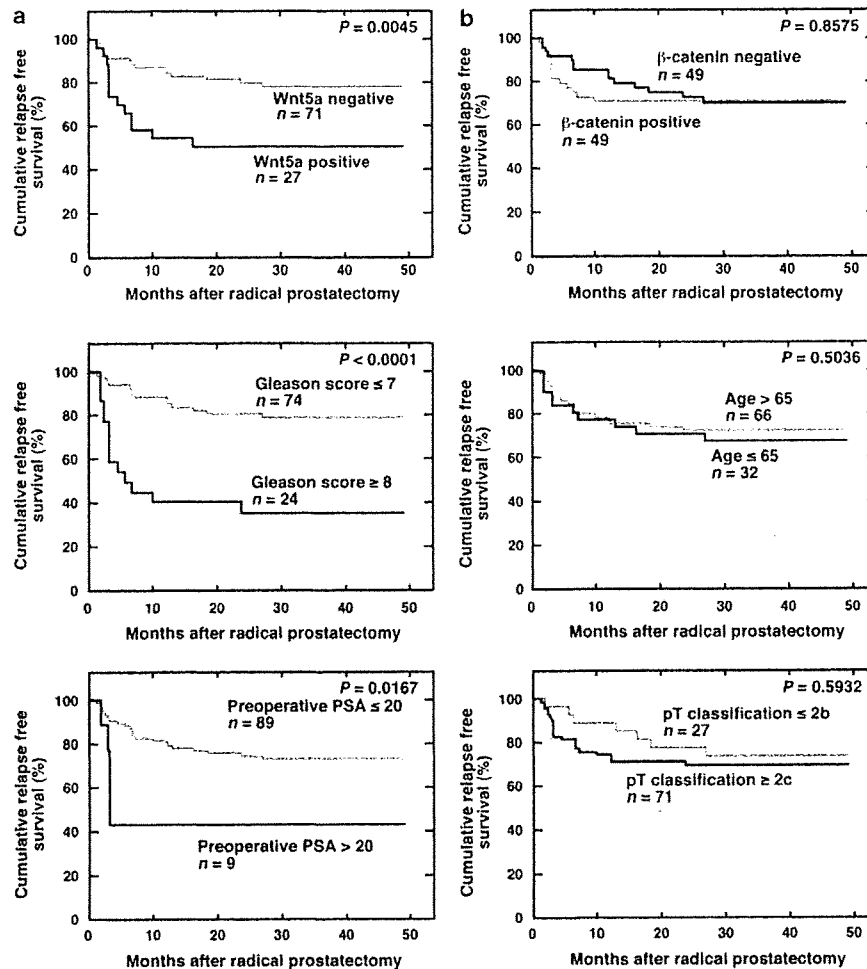


Figure 2 Relapse-free survival of patients with prostate cancer (PCa) expressing Wnt5a or β -catenin. (a) Kaplan–Meier curves of patients with PCa with Wnt5a-negative or Wnt5a-positive PCa (upper panel), with low Gleason score (≤ 7) or high Gleason score (≥ 8) PCa (middle panel), and with low preoperative prostate-specific antigen (PSA) concentration (≤ 20 ng/ml) or high preoperative PSA concentration (> 20 ng/ml) (lower panel). (b) Kaplan–Meier curves of patients with PCa with or without β -catenin expression in the cytoplasm and nucleus (upper panel), with younger (≤ 65) or older (> 65) age (middle panel) and with low pT classification ($\leq 2b$) or high pT classification ($\geq 2c$) PCa (lower panel).

of invasive PCa cells. Frizzled (Fz) family members are known to function as Wnt receptors (Wang *et al.*, 2006). Fz2, Fz6 and Fz7 were expressed highly in DU145 cells compared with other Fzs (Supplementary Figure S2a). Wnt5a bound to Fz2, Fz5 and Fz8 but not to Fz6 and Fz7 (Sato *et al.*, 2010) (data not shown), and Ror2, a single transmembrane protein, is known to function as a Wnt5a receptor (Oishi *et al.*, 2003). To examine which receptor(s) are involved in cell migration of DU145 cells, we depleted Wnt receptors by siRNA (Supplementary Figure S2b). Knockdown of Fz2 and Ror2 but not Fz6 reduced cell invasion by DU145 cells significantly (Figure 4a). Knockdown of Fz7 showed a tendency to decrease cell invasion, but the difference was not statistically significant (Figure 4a). Wnt5a induced the phosphorylation of protein kinase D (PKD)/PKC μ in DU145 cells (Figure 4b). PKD is a protein kinase, which

not only is a direct target of diacylglycerol but also lies downstream of novel PKCs (Rozenfurt *et al.*, 2005). Therefore, these results suggested that Wnt5a activates novel PKCs. Staurosporine, a PKC inhibitor, indeed suppressed Wnt5a-dependent migration and invasion activities of DU145 cells (Figure 4b). Furthermore, Gö6976, an inhibitor that is relatively specific for PKD, suppressed Wnt5a-dependent migration and invasion activities of DU145 cells (Figure 4b). These results suggested that PKD activation by Wnt5a probably through the activation of novel PKCs is involved in Wnt5a-dependent migration and invasion. In addition, Wnt5a activated small G protein Rac, which has a role in cell migration (Figure 4c).

It has been reported that many genes associated with aggressive behavior, including Wnt5a and MMP-9, were increased in androgen-independent metastatic tumors

Table 1 Multivariate analysis of factors influencing relapse-free survival

	Hazard ratio (95% CI)	χ^2	P-value
<i>Wnt5a</i> staining			
Negative	1 (Reference)	3.907	0.0312
Positive	2.451 (1.007–5.960)		
<i>Cytosomal or nuclear β-catenin</i> staining			
Negative	1 (Reference)	1.681	0.1947
Positive	1.782 (0.744–4.265)		
<i>Age</i>			
≤ 65	1 (Reference)	0.101	0.7507
> 65	1.138 (0.513–2.525)		
<i>pT classification</i>			
$\leq 2b$	1 (Reference)	0.161	0.6882
$\geq 2c$	1.215 (0.469–3.148)		
<i>Gleason score</i>			
≤ 7	1 (Reference)	10.976	0.0009
≥ 8	3.912 (1.745–8.769)		
<i>Preoperative PSA concentration</i>			
≤ 20	1 (Reference)	4.574	0.0325
> 20	3.176 (1.101–9.161)		

Abbreviations: CI, confidence interval; PSA, prostate-specific antigen.

and that MMP-1 is involved in invasion by DU145 cells (Stanbrough *et al.*, 2006; Zeng *et al.*, 2006). The stimulation of DU145 cells with Wnt5a increased the expression of *MMP-1* (collagenase) mRNA but not those of *MMP-2* (gelatinase A), *MMP-3* (stromelysin-1) or *MMP-9* (gelatinase B) mRNA, and knockdown of Wnt5a decreased the levels of *MMP-1* mRNA (Figure 5a). Consistent with these results, Wnt5a increased the protein levels of MMP-1 (Figure 5a). As shown in transient expression of Wnt5a in PC3 cells, the invasion activities of PC3 cells were also enhanced by stable expression of Wnt5a, and knockdown of MMP-1 suppressed the invasion activities (Figure 5a). To evaluate the role of Wnt5a on *MMP-1* promoter activity, we transfected the *MMP-1* 5'-flanking region containing two activator protein-1 (AP-1) sites (–517/+60) with luciferase gene into PC3 cells (Figure 5b). Wnt5a increased the promoter activity (Figure 5b). It was reported that the proximal AP-1 site at –72 is necessary for the phorbol ester-induced expression of *MMP-1* (Hall *et al.*, 2003). The basal reporter gene activity was decreased by introducing mutations in this area (*AP-1 mut*), and Wnt5a did not stimulate it (Figure 5b). Consistent with these results, Wnt5a indeed induced the phosphorylation of JNK at Thr183 and Tyr185, which indicates the activation of JNK, in DU145 cells (Figure 5c). In addition, Gö6976 suppressed Wnt5a-dependent JNK activation (Figure 5c), suggesting Wnt5a activates JNK through PKD. c-Jun or JunD has been shown to bind to the AP-1 site in the promoter region of *MMP-1* in MKN45 and U937 cells (Doyle *et al.*, 1997; Wu *et al.*, 2006). In a chromatin immunoprecipitation assay, *MMP-1* promoter occupancy of JunD was decreased in DU145/Wnt5a knockdown cells compared with DU145/control cells (Figure 5d). Furthermore, Gö6976 interfered the binding of JunD to *MMP-1* promoter, but knockdown of Rac did not affect the Wnt5a-induced binding of JunD and *MMP-1* promoter

(Figure 5d). Taken together, these results suggested that Fz2 and Ror2 function as Wnt5a receptors in this signaling of PCa cells and that PKD and JNK mediate Wnt5a-dependent expression of *MMP-1* through the recruitment of JunD to the AP-1 site of the *MMP-1* promoter.

Discussion

Clinical relevance of Wnt5a expression in PCa

PCa is the most commonly diagnosed malignancy, and its incidence is rising in many countries (Hsing *et al.*, 2000; Jemal *et al.*, 2008). The present results showed that the expression of Wnt5a is correlated with a prostatectomy Gleason score ≥ 8 . Gleason score is the most frequently used grading system for PCa and is a powerful prognostic indicator (Gleason and Mellinger, 1974). It has also been reported that prostatectomy Gleason score is a predictor of distant metastasis (Pound *et al.*, 1999). When the Gleason score was ≥ 8 , the probability of distant metastasis was $> 65\%$ at 5 years. In the present cases, patients with a Gleason score ≥ 8 indeed showed a significantly higher risk of biochemical relapse. Furthermore, multivariate analyses showed that the expression of Wnt5a is an independent predictor of biochemical relapse, along with prostatectomy Gleason score and preoperative PSA concentration, indicating that Wnt5a might be a good indicator of the recurrence of PCa. Biochemical relapse indicates the presence of PCa, which may have already migrated to distant sites when the prostatectomy was performed. PCa cells positive for Wnt5a expression could have an ability to invade. Knockdown and overexpression of Wnt5a in PCa cells indeed inhibited and activated, respectively, their migration and invasion activities. Taken together with the observations that sFRP2 and anti-Wnt5a antibody inhibited migration of PCa cells, it is conceivable that Wnt5a is a candidate molecular target of therapy for PCa.

It has been reported that high levels of β -catenin are associated with aggressiveness in PCa (Yardy and Brewster, 2005). Among the current 98 cases, PCa abnormally expressing both Wnt5a and β -catenin was observed in only 5 cases. This is similar to the situation in cases of gastric cancer (Kurayoshi *et al.*, 2006). At present the reason why the expression of Wnt5a and β -catenin is mutually exclusive is not known.

Mechanism by which Wnt5a promotes aggressiveness of PCa

How is Wnt5a involved in the aggressiveness of PCa? Wnt5a increased *MMP-1* mRNA and protein levels in PCa cells, but it did not induce the expression of *MMP-2*, *MMP-3* and *MMP-9* mRNAs. MMPs are zinc-containing endopeptidases that degrade extracellular matrix components and are associated with cancer cell invasion and metastasis (Egeblad and Werb, 2002). It was suggested that upregulation of *MMP-1* is an important factor in the aggressiveness of PCa and bone

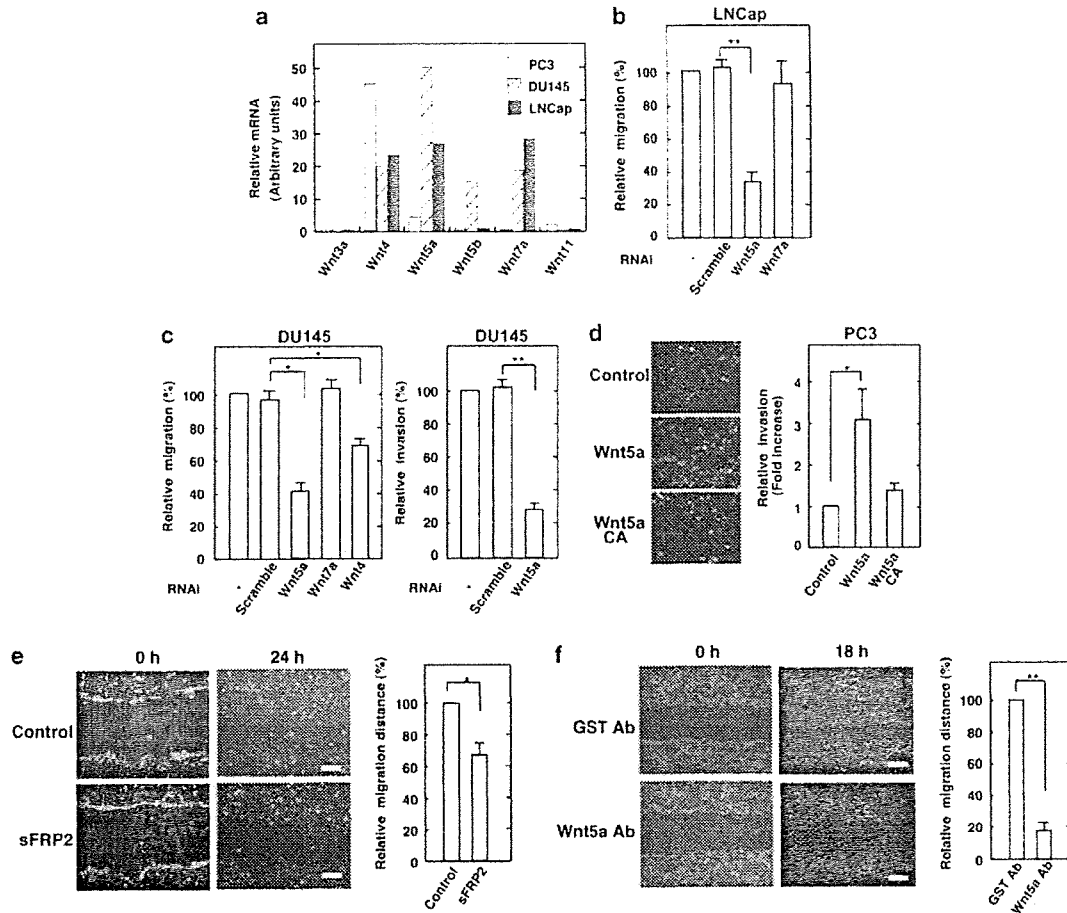


Figure 3 Wnt5a is involved in migration and invasion of prostate cancer (PCa) cells. (a) The mRNA levels of various Wnts in PC3, DU145 and LNCap cells were quantified by quantitative reverse transcription (RT)-PCR. (b) LNCap cells transfected with *scrambled* (control), *Wnt5a* or *Wnt7a* siRNA were placed in transwell chambers for a migration assay toward fibronectin. In three independent fields, 130 ± 7 untransfected cells transmigrated. Relative migration activities were expressed as percentages for the migration of untransfected cells. The results shown are means \pm s.e. from three independent experiments. $**P < 0.01$. (c) DU145 cells transfected with *scrambled*, *Wnt5a*, *Wnt7a* or *Wnt4* siRNA were placed in noncoated (left panel) or Matrigel-coated (right panel) transwell chambers for migration and invasion assays. In three independent fields, 189 ± 11 untransfected cells transmigrated and 34 ± 6 untransfected cells invaded. Relative migration and invasion activities were expressed as percentages for the migration and invasion of untransfected cells. $*P < 0.05$; $**P < 0.01$. (d) Left panel, PC3 cells transfected with pPGK empty vector (control), pPGK/wild-type Wnt5a (Wnt5a) or pPGK/Wnt5a^{C104A} (Wnt5a CA) were placed in Matrigel-coated transwell chambers for an invasion assay. Right panel, in eight independent fields, 22 ± 12 of PC3 cells transfected with empty vector invaded. Relative invasion activities were expressed as fold increases compared with the invasion of transfectants with empty vector. $*P < 0.05$. (e) Control or secreted Frizzled-related protein 2 (sFRP2) conditioned medium (CM) was added to DU145 cells and then the cells were wounded. The culture was further continued for 24 h. Bars, 200 μ m. Right graph, migration distances were measured and expressed as percentages of the migration in the presence of control CM. $*P < 0.05$. (f) DU145 cells incubated with anti-glutathione *S*-transferase (GST) or anti-Wnt5a antibody (10 μ g/ml) were wounded. The culture was continued for 18 h. Bars, 200 μ m. Right graph, migration distances were measured and expressed as percentages of the migration in the presence of anti-GST antibody. $**P < 0.01$.

marrow metastasis (Hart *et al.*, 2002). This study showed that knockdown of MMP-1 indeed suppressed Wnt5a-dependent invasion of PC3 cells *in vitro*.

Although how MMP-1 is overexpressed in PCa is not clear, one report showed that a pathway involving FAK, PI3K and PKC δ activated by engagement of integrin $\alpha 5 \beta 1$ with fibronectin regulates the expression of MMP-1 in DU145 cells (Zeng *et al.*, 2006). It was also shown previously that Wnt5a induces the expression of MMP-1 in endothelial cells although the mechanism was not

known (Masckauchan *et al.*, 2006). This study found that Wnt5a induces the phosphorylation of PKD/PKC μ , which is a direct target of novel PKCs (PKC δ , PKC ϵ , PKC η and PKC θ), and activates JNK. Furthermore, it was shown that Wnt5a signaling recruits JunD to the AP-1 site of the *MMP-1* promoter region. These results were consistent with the previous observations that the AP-1 site in the promoter region of the *MMP-1* gene is critical for its transcriptional regulation (Angel *et al.*, 1987) and that c-Jun and JunD bind to the AP-1